/o 2

Reprinted from

GEOCHIMICA ET COSMOCHIMICA ACTA

Journal of the Geochemical Society

On the unity and origin of the Australasian tektites

Dean R. Chapman

National Aeronautics and Space Administration, Ames Research Center
Moffett Field, California

3/57/

Abstract—Aerodynamic experiments with tektite glass demonstrate that, subsequent to the termination of ablation, high thermal stresses are formed within a thin outer shell. This shell spontaneously spalls, leaving a core shaped like many of the tektites found in Billiton, Java, Philippines and Australia. Certain tektite fragments from Java and Australia are shown to have the same internal stress patterns as pieces of aerothermal stress shell. The over-all evidence indicates that the Australasian tektites descended into the atmosphere as *rigid* objects of glass.

Core shapes found in the extreme southwest part of Australia surprisingly are more like those found in the Philippines than in other areas of Australia; comparisons of chemical analyses and of specific gravity population polygons reveal the same striking circumstances. It is concluded that all Australasian tektites represent a single event.

A study of tektite forms, in relation to results from laboratory experiments, indicates that the temperature of formation of primary shapes varied progressively across the Australasian strewnfield. The sculpture on certain australites provides a record of tumbling during entry into the Earth's atmosphere. The effect of turning on the determination of entry trajectories is discussed, and new evidence is presented pertaining to the deceleration which existed when ablation terminated on the australites. The trajectory determinations correspond to an origin from the Moon.

Numerous trajectories from the Moon to Earth have been studied with a high-speed electronic digital computer. The relative probability of such trajectories is about 1/200 for the Moon as a whole, and 1/60 for certain crater locations. A comparison of the geographical spread of the Australasian tektites with the Earth landing patterns for lunar material ejected within the azimuthal dispersion observed of lunar rays, and within the elevational dispersion measured in hypervelocity impact experiments, indicates mutual compatibility.

INTRODUCTION

New evidence pertaining to the formation of tektites has been obtained from several different methods of investigation. One source of evidence is based on observations of tektites made during a field trip in Sept.–Dec. 1962 to Australia, Indonesia, southeast Asia and the Philippines. In order to provide a basis for interpreting this observational evidence, various laboratory experiments and analytical investigations have been conducted. These pertain mainly to phenomena encountered by tektites during entry into the atmosphere. Since a considerable body of physical evidence has pointed to trajectories coming directly from the Moon as the path of tektite flight (Chapman and Larson, 1963) computations have been made of a number of such trajectories starting from various places on the Moon. These rather diverse topics—field observations, laboratory aerodynamic experiments, and Moon–Earth trajectory calculations—are described in separate parts of this paper.

Among the many different groups of Australasian tektites, only the australites and javanites heretofore have been proven to exhibit unmistakable aerodynamic evidence. Since these two groups comprise less than 10 per cent of the Australasian

tektites, an important question arises as to why the vast majority of these tektites does not exhibit equally plain aerodynamic evidence. The apparent absence of ablation markings on tektites from the Philippines, southeast Asia and Billiton has led some scientists to presume that these tektites, unlike the australites and javanites were not ablated as rigid bodies during a hypervelocity descent into the atmosphere; and, hence, must have been formed somewhere near the northern areas of the strewnfield rather than far away. Consequently, it was one of the principal objectives of the field trip to look for aerodynamic evidence on tektites from these areas.

From observations that a certain type of tektite core is found throughout Australasia, a lead was obtained on the form which aerodynamic evidence takes on such tektites. In order to investigate this evidence more thoroughly, various thin sections were sliced from tektites and from models ablated by aerodynamic heating. A study of these sections, as developed in part I of this paper, provides an explanation of what has happened to the aerodynamic evidence on tektite cores. Inasmuch as these results lead to a unified picture of rigid-body ablation on all of the tektites scattered from Australia to the Philippines, various other evidence is discussed in part I which pertains to the unity of the Australasian tektites. This latter evidence is drawn from tektite sculpture, chemical composition, and specific gravity population polygons.

In part II of this paper, some new results pertaining to the atmosphere entry analysis of australites are presented. These results, obtained subsequent to a previous publication (*ibid.*), relate to the effects of pre-entry turning on the amount of ablation, the effect of body forces on ring-wave spacing, and the effect of deceleration on flange flattening. Such effects have a significant bearing on the determination of entry trajectories—and hence origin—of the tektites; and their inclusion in the atmosphere-entry analysis enables sharper limitations on entry trajectories to be obtained than in previous investigations.

The hypothesis of tektite origin through direct Moon-to-Earth trajectories has never been enthusiastically received, and numerous "objections" to such an origin have been advanced. But no hypothesis of tektite origin has appeared fully satisfactory, and the tektite literature is full of objections to all suggested origins. Many such objections appear to be based more on intuitive expectations than on either rigorous calculations or experimental observations. In the case of direct origin from the Moon, two such objections are that the estimated probability is too low, and the expected geographical distribution is wrong. It is the author's view that such an origin has been too hurriedly dismissed on these grounds, especially in a recent paper by UREY (1962). Consequently, in order to determine whether such objections are valid, numerous calculations on a high-speed electronic digital computer have been made of Moon-to-Earth trajectories. These results are presented in part III of this paper.

Throughout this paper an abbreviation is used in identifying the tektite collection associated with each specimen individually referred to. A specific tektite is identified by the museum or collection number prefixed by one of the following abbreviations:

       A.M.   Australian Museum, Sydney
       G.B.   George Baker collection, Melbourne
       G.M.M.   Geological and Mining Museum, Sydney

N.M.V.   National Museum of Victoria, Melbourne
N.A.   NASA Ames Research Center, Moffett Field, Calif.
R.G.M.   Rijksmuseum van Geologie en Mineralogie, Leiden
S.A.M.   South Australian Museum, Adelaide
U.M.G.D.   University of Melbourne Geology Department, Melbourne
U.S.N.M.   United States National Museum, Washington, D.C.
V.K.   von Koenigswald Collection, Utrecht
W.A.M.   Western Australian Museum, Perth

PART I. UNITY OF AUSTRALASIAN TEKTITES

UNITY OF CHEMISTRY

Previous studies of the chemical composition of Australasian tektites are summarized in the recent papers of CHAO (1963) and SCHNETZLER and PINSON (1963). In these studies tektite analyses from different countries have been compared rather thoroughly, although without a specific guide as to which areas within Australasia might correspond to common populations. The geographic distribution of these tektites is illustrated on the map of Fig. 1. The objective of this section is to compare analyses reported in the literature for the Manila Bay tektites with analyses for the australites from southwest Australia. These two particular areas have the same population polygon of specific gravity (CHAPMAN, LARSON and SCHEIBER, 1963). Hence, if the interpretation is correct that tektites from these two widely separated areas originated from a common batch mixture that was melted, disrupted, and then widely strewn, it would be anticipated that they also should exhibit a common composition, at least of the major chemical elements.

Table 1 presents a compilation of chemical analyses pertinent to the present objective. In the two columns at the left of this table, the average of 17 analyses available for Manila Bay tektites is compared with the average of 7 analyses available for australites from southwest Australia. It is evident that the average major-element chemistry of these two tektite groups is virtually the same, even though the distance between the two areas spans almost the entire Australasian strewnfield. Moreover, this close correspondence of chemistry between Manila and southwest Australia also is reflected in individual analyses of tektites having the same silica content, as may be seen by comparing in Table 1 the third column representing a Manila Bay philippinite of 69·3 per cent silica with the fourth column representing a southwest australite of 69·0 per cent silica. Both of these analyses (3965 from Santa Mesa, Manila, and 4215 from Nullarbor Plains) were made in the same laboratory by Schnetzler and Pinson.

The observed coincidence of tektite chemistry between two widely separated localities which also exhibit coincident population polygons of specific gravity demonstrates that, among the many distinguishable clusters which showered over the Australasian portion of the globe, at least one was dispersed from essentially the northern to the southern extremity of the strewnfield. The congruity of tektite populations in Manila Bay and southwest Australia leads to a certain interpretation in the light of contrasting differences observed between tektite clusters found relatively close together in Australasia. From our population polygons it has been

established that much greater differences commonly exist between the clusters in a given country than between either southwest Australia and Manila, or between central Australia (Charlotte Waters) and Java. There is additional chemical evidence pointing to the same odd circumstances: the chemical analysis given in Table 1 for
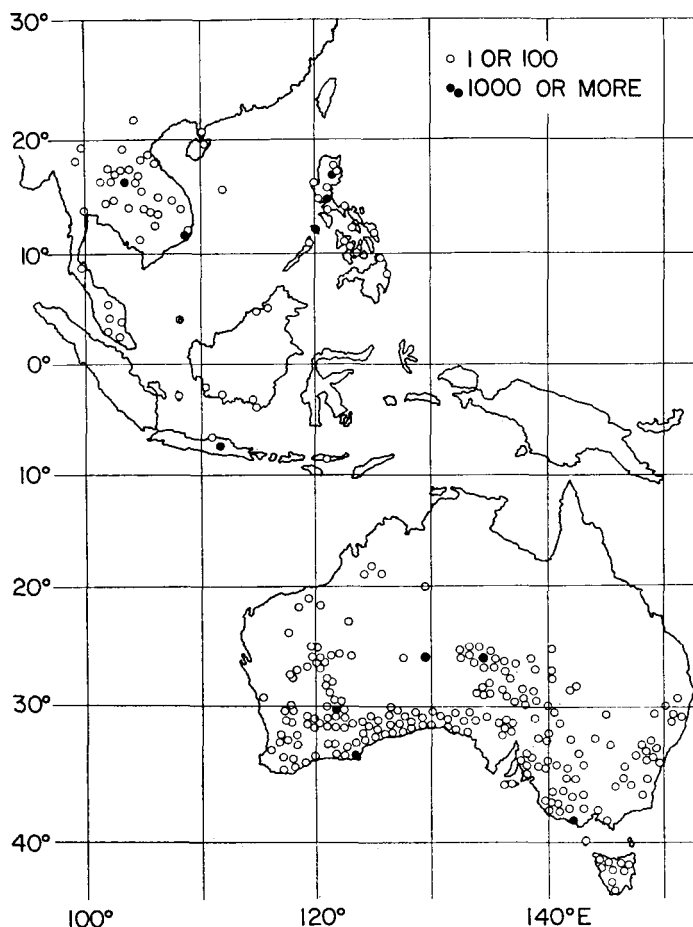

Fig. 1. Distribution of Australasian tektites.

Florieton, which corresponds to a silica content typical for southwest Australia, differs greatly from a typical analysis from southeast Australia, yet is strangely close to the analysis of a Muong Nong tektite in Thailand, some 7000 km away. A tentative interpretation of these circumstances is that the Australasian tektite swarm arrived near the Earth in the form of many distinguishable clusters, some of which were strung out in an interrupted string-like fashion over lengths comparable to the maximum expanse of the Australasian fall (the order of several thousand kilometers), while being spread in width over dimensions comparable to the minimum distance between localities which exhibit clearly distinguishable population polygons (the order of several hundred kilometers).

Table 1. Some chemical analyses of Australasian tektites

| | Averages | | | Individual analyses | | |
	Manila $a(13) + c(4)$	S.W. Aust. $b(7)$	Manila a	N.P. Aust. a	Florieton Aust. b	Muong Nong d
SiO_2	70·8	71·0	69·3	69·0	76·7	76·9
Al_2O_3	13·8	13·0	14·9	15·3	10·5	10·6
Fe_2O_3	0·6	0·4	0·5	0·4	0·8	0·6
FeO	4·4	4·5	4·8	4·5	3·6	3·3
MgO	2·6	2·3	2·8	2·3	1·6	1·6
CaO	3·1	3·2	3·3	3·2	2·4	1·6
Na_2O	1·4	1·4	1·3	1·6	1·1	1·4
K_2O	2·4	2·5	2·5	2·5	2·1	2·3
TiO_2	0·8	0·8	0·8	0·8	0·6	0·7
	5000 km			1300 km	7000 km	

[a] Schnetzler and Pinson (1963).
[b] Taylor (1962).
[c] Chao (1963), analyst Cuttitta.
[d] Barnes and Pitakpaivan (1962), analysts Elmore Barlow, Botts and Chloe.

CONTINUITY OF TEKTITE CORE SCULPTURE ACROSS AUSTRALASIA

A picture of the mechanism by which tektite cores were produced has been developed from observations of the formation and behavior of an aerothermal stress shell. Such a shell is produced in the latter stages of an entry flight as the front face is rapidly cooled to temperatures below the strain temperature of tektite glass. Under certain conditions of size, of entry trajectory, and of tektite composition, this shell spontaneously spalls, leaving a tektite core. When the aerodynamic trajectory factors affecting the aerothermal stresses are considered together with the subsequent effects of prolonged terrestrial etching, an explanation is obtained for the existence of a common type of tektite core throughout Australasia. An outline of the evidence leading to this interpretation is developed in the present section.

Aerothermal stress shell

That severe residual thermal stresses are induced within an outer shell under the front face of a tektite during the latter stage of its descent through the atmosphere may be illustrated from computations of the temperature distribution at various intervals of time after aerodynamic ablation terminates. An example is presented in Fig. 2 for the following conditions: initial entry velocity $V_1 = 11$ km/sec, initial entry angle $\gamma_1 = 30°$ from the horizontal, and tektite glass of density $\rho = 2·40$ g/cm³. In making such calculations, as noted elsewhere (CHAPMAN and LARSON, 1963), the transport of heat by internal radiation and thermal conduction is computed as a function of time during the entire entry flight. Also, the corresponding variations in flight velocity, atmosphere density, flight-path angle, ballistic drag parameter ($m/C_D A$, where m = mass, C_D = drag coefficient, and A = projected frontal area), and front surface radius of curvature R_F automatically are calculated as a function of
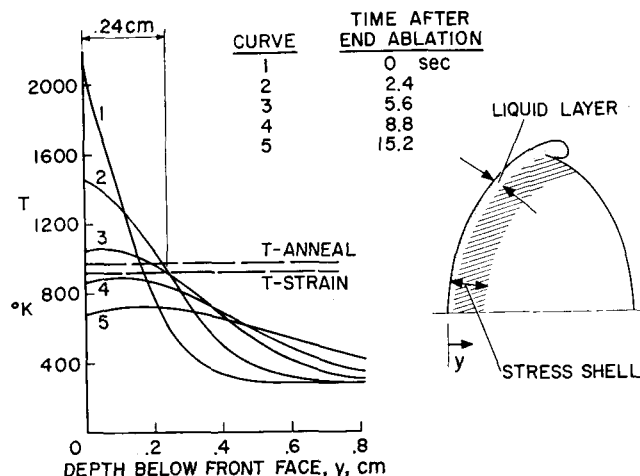
Fig. 2. Temperature distribution along axis of symmetry for various times after ablation terminates in flight; $V = 11$ km/sec, $\gamma_i = 30°$.

time by a high-speed digital computer (IBM 7094) programmed to solve simultaneously the combined system of differential equations of aerodynamic ablation and of trajectory motion. The post-ablation temperature history along the axis of symmetry as illustrated in Fig. 2, is characterized by rapid cooling of the front face. For tektite glass of density $\rho = 2\cdot40$, the strain temperature is about $650°C$ ($923°K$), and the annealing temperature, about $700°C$ ($973°K$). When decreasing through this annealing temperature range the temperature variation is large, and the front-face surface temperature in the particular example illustrated is cooling at about $58°C/$ sec—such conditions would induce pronounced thermal stresses within a shell under the front surface. Since the strain temperature represents the temperature up to which a glass may be heated and rapidly cooled without inducing residual strain, it is seen from Fig. 2 that the aerothermal stress shell would extend in this particular example to a depth t_s of about $2\cdot4$ mm. Since the front layer is heated well above the annealing temperature and solidifies at dimensions commensurate with the relatively cool and rigid interior, it develops tensile stresses as it further cools to ambient temperature. Tensile stresses in glass, of course, are prone to structural failure.

The pattern of aerothermal stresses would be compounded with any other stresses existing prior to entry. An initial stress pattern is established when the primary tektite shapes cool in space subsequent to their fusion during formation. (It has been demonstrated previously that the formation of essentially undeformed spheres of molten tektite glass, such as represented by some of the primary australites, must have taken place in a near vacuum (*ibid.*, pp. 4315–4324).) Also, a localized stress pattern is formed around chemically inhomogeneous inclusions and striae bands. In some tektites the aerothermal stresses are considerably obscured by these other stresses.

As might be anticipated, the entry angle into the atmosphere has an important effect on the thickness of the aerothermal stress shell and on the magnitude of the residual thermal stresses. For steep entry the duration of heating is short, the stress shell thin, and the rate of cooling rapid. The results of computations similar to those

presented in Fig. 2, only for various entry angles, illustrate these circumstances (γ_i is measured relative to the horizontal; $V_i = 11$ km/sec).

Entry angle γ_i, deg	Thickness of stress shell, t_s, mm	Cooling rate of front face in annealing range (dT_s/dt), deg/sec
6	4·0	21
20	2·7	49
30	2·4	58
45	2·1	80
90	1·8	120

From these results it is to be expected that the residual aerothermal stresses will increase as the descent becomes steeper. It is important to note, however, that the results tabulated above and the features exhibited by the temperature profiles in Fig. 2 are representative of tektites of core size, or of large buttons, but not of small buttons or lenses. Within a small tektite, especially for relatively shallow descents, the front and base heating profiles merge, the tektite is heated throughout to temperatures above the strain temperature, and the aerothermal stress pattern extends from front to base. Under such circumstances the clearly demarked, thin, aerothermal stress shell characteristic of core-size tektites would not exist. Only for a very steep entry would such a shell be found on small tektites.

The thermal stress patterns induced by aerodynamic ablation are prominently displayed when a thin section is placed between cross-polarized sheets. Aerothermal stresses are clearest when produced in synthetic tektite glass, because such glass is essentially free from secondary stresses associated either with chemical inhomogeneities or with a first period of melting. Some instructive examples are illustrated in Fig. 3. Each section is a meridional one of constant thickness (0·5 or 1·0 mm), oriented so that the relative air stream would be from left to right. Stresses are revealed by the presence of light areas, since unstressed glass would appear dark under cross-polarization. Examples in the top row represent synthetic tektite glass models ablated by aerodynamic heating in an arc jet ((a) is model STG-2S, (b) is SJ-E and (c) is SJ-C); while examples in the lower row represent natural tektites ((d) and (e) are Sangiran javanites obtained from G. H. R. von Koenigswald and (f) is a Nullarbor Plains australite obtained from the American Meteorite Laboratory). It is important to note that the lens-shaped areas at the base of models (a) and (b) remain dark as these sections are rotated in their own plane; such areas, therefore, have not been stressed by aerodynamic heating. In example (a) the thickness of the aerothermal stress shell is seen to be about 2 mm and in example (b) about 3 mm. From the observed systematic curving of several striae near the front face in the upper portion of section (b), the liquid layer is seen to have been a fraction of a millimeter thick. Thicknesses of several tenths of a millimeter for the liquid layer and several millimeters for the aerothermal stress shell are typical for conditions of tektite ablation. Section (c), in contrast to (b), exhibits an aerothermal stress pattern throughout its 7 mm depth, so that in this case, there is no clearly demarked stress shell. The difference between (b) and (c) is due to different aerodynamic heating conditions; (b) was

7

heated at a higher rate for a shorter time (stagnation enthalpy of 2100 cal/g for 11 sec) than was (c) (1400 cal/g for 20 sec). They were cooled under similar conditions after ablation terminated; hence, the slower rate and longer heating resulted in a deeper penetration of the thermal stresses. In an entry flight short heating pulses arise from steep entry angles or high entry velocities, and are accompanied by high rates of cooling following the termination of ablation. It follows, therefore, that the javanites in Fig. 3 definitely have been heated for a shorter time during atmospheric entry than has the australite. The interpretation of this result is that the javanites entered the atmosphere at a steeper angle than the australite.

Some variables other than entry angle which affect the magnitude of thermal stresses and the thickness of the stress shell should be recognized. For a given modulus of elasticity, the residual thermal stress will increase with an increase either in the coefficient of thermal expansion α or the characteristic dimension L. The stress increases with size because both t_s and the temperature change from annealing to ambient are nearly independent of size, while shrinkage during cooling is proportional to αL., and stress to $\alpha L/t_s$. The principal variable affecting α is the silica content: α(cm/cm°C increases from 7×10^{-7} for pure silica to about 29×10^{-7} for tektite glass of 80 per cent silica, to 42×10^{-7} for 65 per cent silica. Shrinkage proportional to αL implies that for sufficiently small tektites the thermal stresses will be within the strength limit of the glass, while for sufficiently large tektites they will exceed that for fracture. In view of the earlier comments about the effect of entry angle, it is to be expected, therefore, that large tektites of low silica content descending steeply into the atmosphere will experience some form of spontaneous fragmentation, or spallation, of the aerothermal stress shell; and that this would extend to depths of several millimeters below the surface at the stagnation point.

Natural spallation leaves core shape and removes principal aerodynamic evidence

Ample evidence that the aerothermal stress shell spontaneously spalls from core-size tektites, is provided by laboratory experiments and by tektite observations alike. As illustrated in Fig. 4, one-half of the stress shell sometimes spalls, leaving a clear indication both of the stress shell profile and the core shape which would be produced if the remaining half of the shell also were to spall from the core. Examples of half spallation have been observed in most of the tektite collections in Australia. The natural tektite in Fig. 4 represents G.B. 1406, a Port Campbell australite with $R_B = 1\cdot2$ cm and $\rho = 2\cdot37$ (approximately 80 per cent silica). On well-preserved australites that are somewhat larger than G.B. 1406, or lower in silica content, the spallation is more complete, and only small portions of the stress shell, called "indicators" by Fenner, remain attached to the core. An excellent example of this is provided by S.A.M. 622 illustrated in three views in the lower row of Fig. 5. Also shown for purposes of comparison is one of our models (STG1-S) from which five pieces of stress shell spalled. This model was ablated at a higher heating rate and for shorter duration than the model in Fig. 4 which only half spalled. Still larger tektites than S.A.M. 622, such as the three illustrated in Fig. 6, invariably reveal that complete spallation occurs; no portion of the aerothermal stress shell remains attached to these large cores. Stress shell spallation would occur either late in flight after ablation terminated, or upon landing (the larger the size, the greater the

terminal velocity of fall, and the more severe is the impact upon striking the Earth's surface).

A particularly informative australite core is W.A.M. 4455, represented in three views at the top of Fig. 6. This is the largest australite (218 g) examined by the author, and, prior to a recent find of a 238 g specimen described by Baker (1962) was regarded as the largest australite known. Two characteristic features of well pre-served tektite cores are exhibited clearly by this specimen: (1) a sharp equatorial rim produced when the stress shell fractured from the core; and (2) an essentially different type of sculpture on the opposite faces of the lens-like core. It is concluded that the many "worm grooves" on the face from which the stress shell spalled (view at top left in Fig. 6) definitely are the result of prolonged terrestrial exposure, for such grooves are not observed in any of our experiments wherein the spallation is fresh; and they could not have been produced by aerodynamic phenomena, since the entire aerothermal stress shell containing the aerodynamic markings—including flow waves and systematically distorted striae—has spalled away. That these worm-like grooves occur selectively on the side which faced forward during flight, rather than on the base, is attributed to a selective etching of the spalled face which contains different stresses than the posterior surface which did not spall. It is emphasized that such grooves, which are common on billitonites and philippinites, are also clearly exhibited on some australites. The only difference is one of degree, either in prevalence or in size of the worm grooves, and this may be attributable mainly to different geological environments during the period of prolonged etching, coupled perhaps with differences in angle of entry into the Earth's atmosphere.

The principal point illustrated by the photographs of three cores in Fig. 6 is that there is no real difference in the external form of, or the aerodynamic evidence revealed by, tektite cores from either Billiton (B in Fig. 6), the Philippines (P), or Australia (A). There is clearly some aspect of unity behind the presence of such strikingly similar shapes from the southern to northern extremities of the Australa-sian strewnfield. For a given size and silica content, cores without any portion of the aerothermal stress shell attached are apparently universal in the Philippines and Billiton, dominant in Java, and less prevalent in Australia. One interpretation of this, compatible with the aerodynamic evidence for lunar origin of the australites, is simply that the angle of entry of the tektite swarm was steeper in Java and regions farther north, than in the southern regions. Under such circumstances, the aero-thermal stress shell would have spalled from all tektites but those of very small size (less than 1 cm, judging from the javanite evidence); and, being only a few milli-meters thick, this shell would have been etched into oblivion in regions such as Billiton and the Philippines where the extent of etching, as measured by the width of deep U-grooves, typically is the order of 1 or 2 mm.

In view of the evidence that a shell of several millimeters thickness has spalled from most Australasian tektites, it is to be expected that fragments of these shells should be found in those areas where terrestrial etching and abrasion have not been too great. Numerous fragments of stress shell are, in fact, found in tektite collections in Australia, especially in that of the South Australian Museum which includes several hundred such fragments (many from the Nullarbor Plain). The largest stress shell fragments that the author has seen, however, are from Sangiran, Java. These

are illustrated in Fig. 7. Among a handful of fragments obtained from one individual at Sangiran, the three largest were found to have the same specific gravity (2·4355 ± 0·0005) and to fit mutually together into a shield-like shell. The assembly of pieces indicates that they spalled from a rather large tektite (Fig. 7). Since the mating edges exhibit a pronounced etch pattern of internal striae, as pronounced as on almost any javanite surface, it is certain that the fragmentation took place long ago. Since they were found in mutual proximity, and since the wave crests are sharp on the irregularly meshed pattern of aerodynamic flow ridges covering the convex side of each fragment, it follows that the fragmentation took place either upon landing, or shortly thereafter, and that terrestrial transportation of these javanites could not have been very great.

Thus far it has been demonstrated from observations of external sculpture that the principal aerodynamic evidence is removed from a tektite when the stress shell spalls. Observations of internal structure fully confirm this view, as may be seen from the thin sections in Fig. 8 which were photographed between cross-polarized sheets. The crack visible in thin-section (a), which was sliced from a model ablated by aerodynamic heating, clearly outlines the form spallation has taken in this case. A precisely similar form of spallation from an australite fragment (S.A.M. 743, Nullarbor Plains) is represented by thin-section (b). Clearly, the pronounced aerothermal stress bands, the ring waves, the flanges, and the systematically disturbed striae, all are removed along with the shell when it spalls off. Thin-section (c) corresponds to a model of synthetic tektite glass that was heated at a high rate for a short time, and extensively spalled upon being cooled. A portion of stress shell which spalled has been replaced in its original position. This shell is rather thin and reveals an unusually close spacing between fringes; as would be anticipated for conditions of high thermal stress. The dark core shape is characteristic of the lens-like shape with sharp equatorial rim that is found on well preserved tektite cores. Since this core region remains dark as the thin section is rotated in its own plane between the cross-polarized sheets, it has not been stressed appreciably by the aerodynamic heating on the front face. Thin-section (d) in Fig. 8 has been sliced from one of the fragments of javanite spallation shell photographed in Fig. 7, and clearly reveals that the characteristic stress bands associated with aerodynamic heating have been removed with this shell when it spalled off, as have been the waves of flow ridges and the thin melt layer just underneath the flow ridges. It cannot be expected, therefore, that tektite cores formed by spallation will reveal any direct aerodynamic evidence. Meridional thin sections of four such cores, one from Australia one from Billiton Island and two from Isabela, Philippines, as illustrated in Fig. 9, reveal the same general pattern of over-all strain. Such patterns are not those induced by severe aerodynamic heating on the front face, but may be either those produced upon cooling in space after the first heating or those induced by the aerodynamic heating on the base surface. These mutually similar patterns clearly point to a common history of formation for australite, billitonite and philippinite cores.

Continuity of tektite core sculpture

From observations of many thousands of Australasian tektites it has been

cm

(a)   (b)   (c)

AERODYNAMIC ABLATION

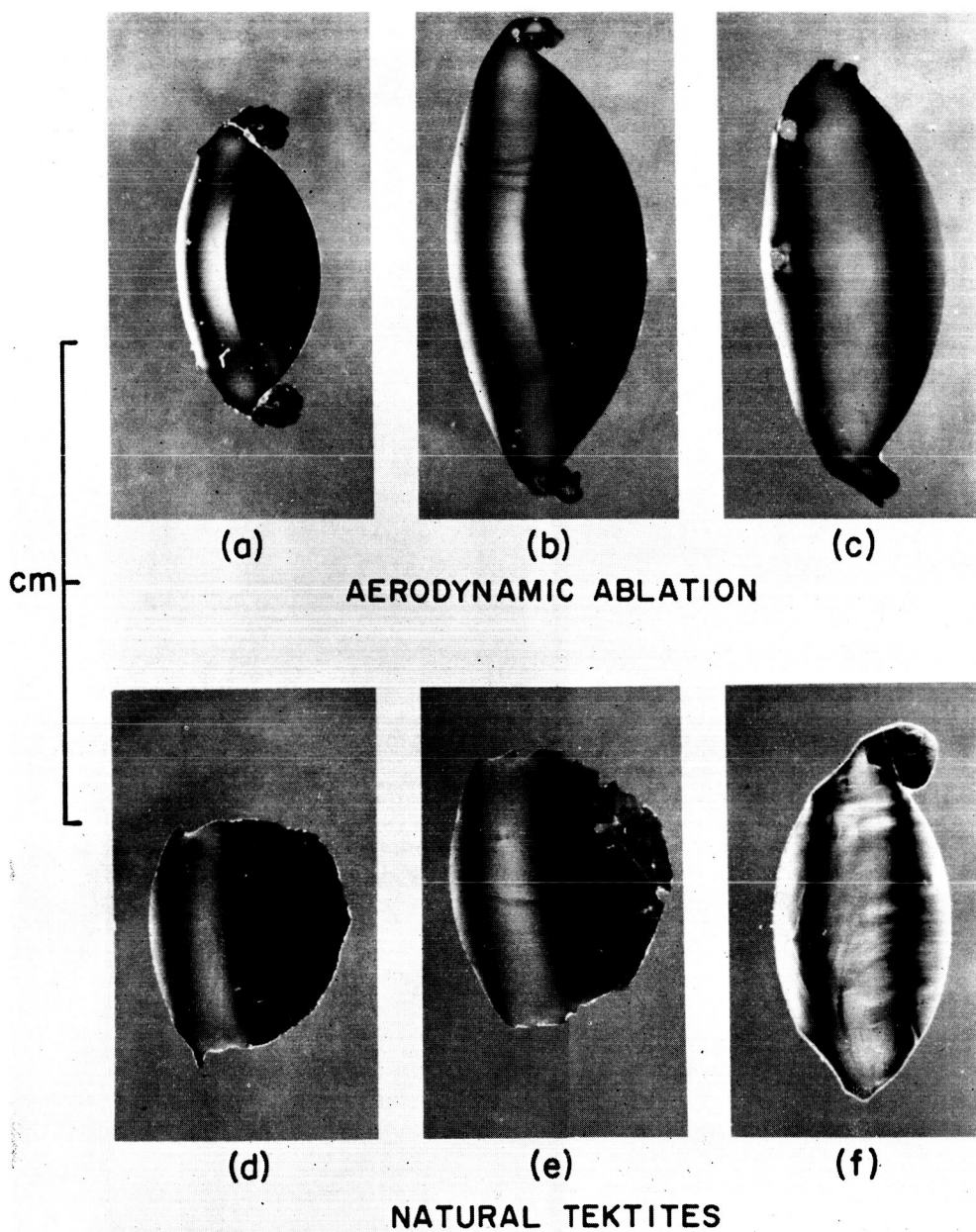(d)   (e)   (f)

NATURAL TEKTITES

Fig. 3. Thin sections in cross polarized light of models ablated by aerodynamic heating compared with natural tektites: (a, b, c) synthetic tektite glass; (d, e) javanites from Sangiran; (f) australite from Nullarbor Plains.
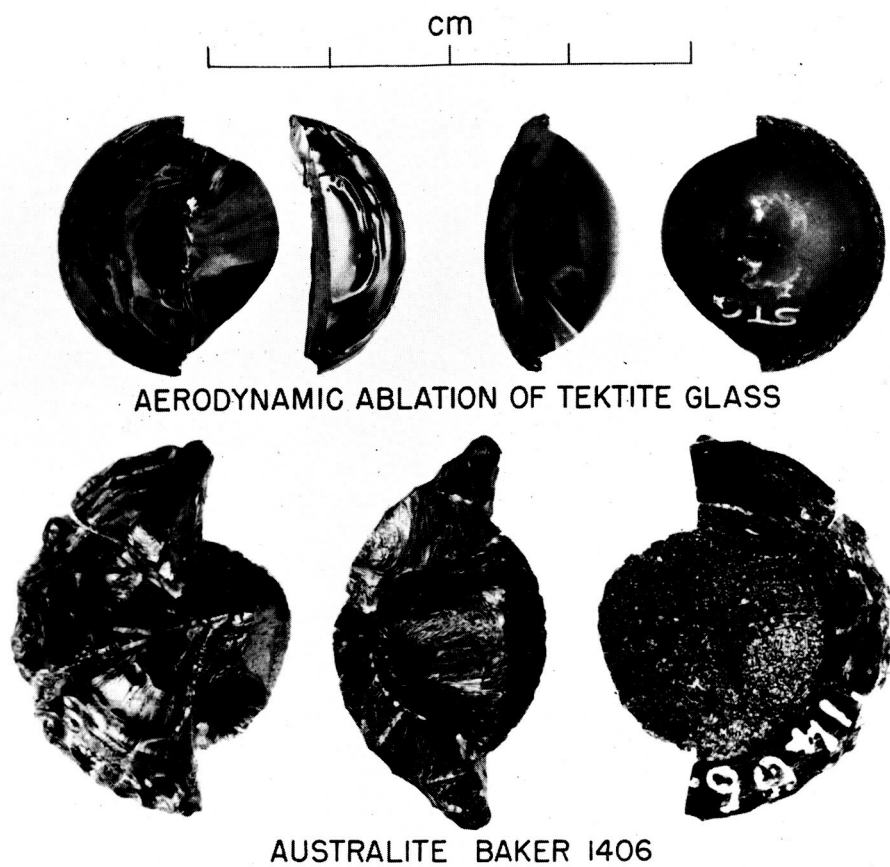
cm

AERODYNAMIC ABLATION OF TEKTITE GLASS

AUSTRALITE BAKER 1406

Fig. 4. Half spallation of aerothermal stress shell.

AERODYNAMIC ABLATION OF TEKTITE GLASS

cm

AUSTRALITE   S. A. M. 622

Fig. 5. Nearly complete spallation of aerothermal stress shell.
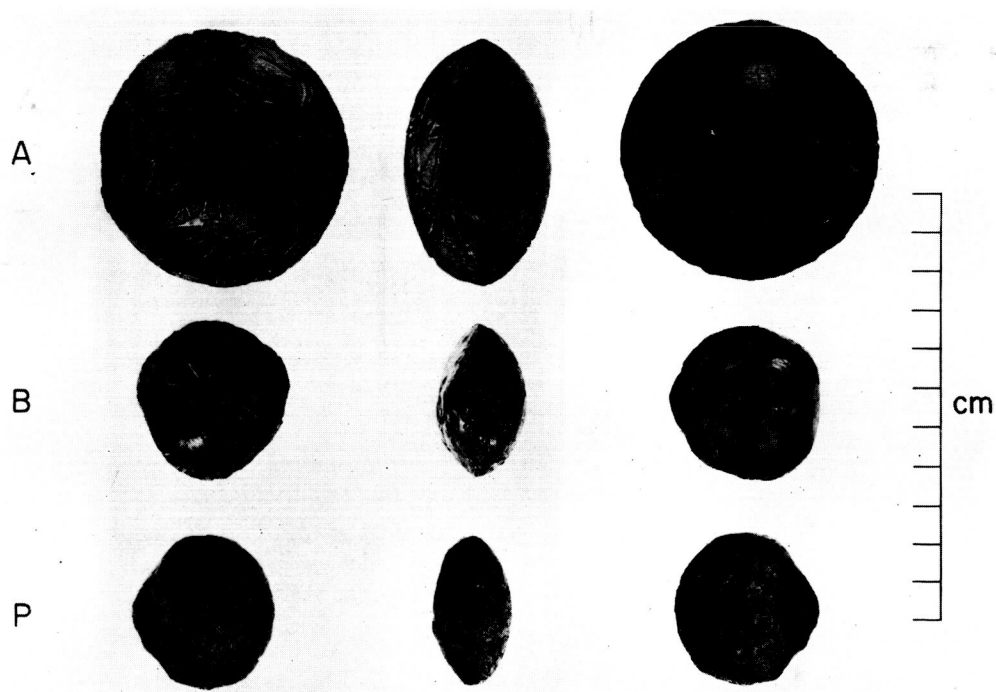

A

B

cm

P

Fig. 6. Australasian cores with smoothly curved base and complete spallation of aerothermal stress shell (A = W.A.M. 4455 from Lake Yealering, Western Australia; B = U.S.N.M. 77761 from Billiton; P = U.S.N.M. 1915 from Isabela, Philippines).
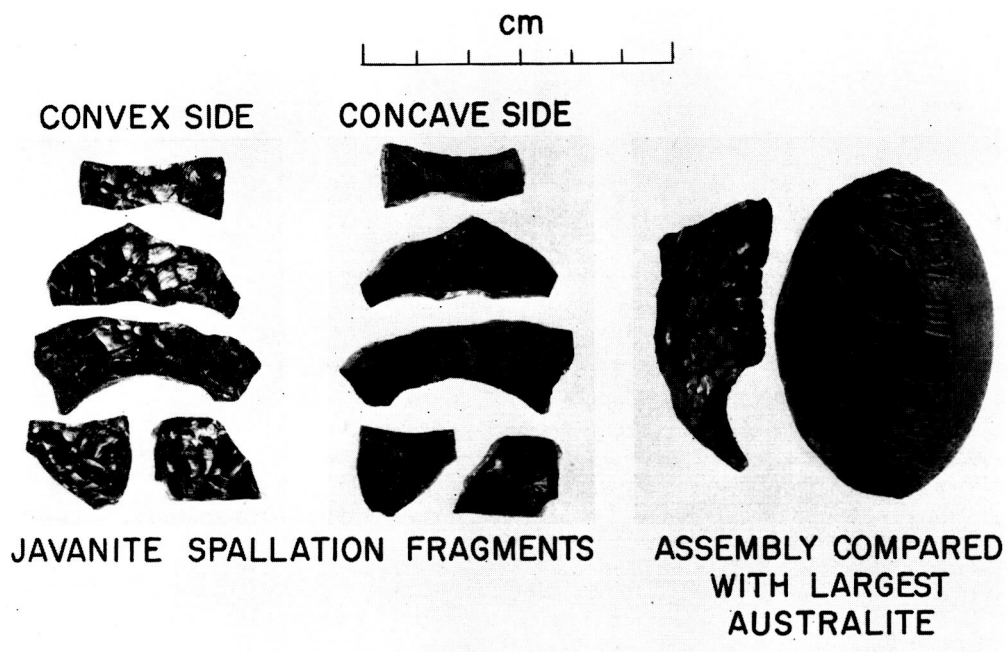
cm

CONVEX SIDE   CONCAVE SIDE

JAVANITE SPALLATION FRAGMENTS   ASSEMBLY COMPARED
WITH LARGEST
AUSTRALITE

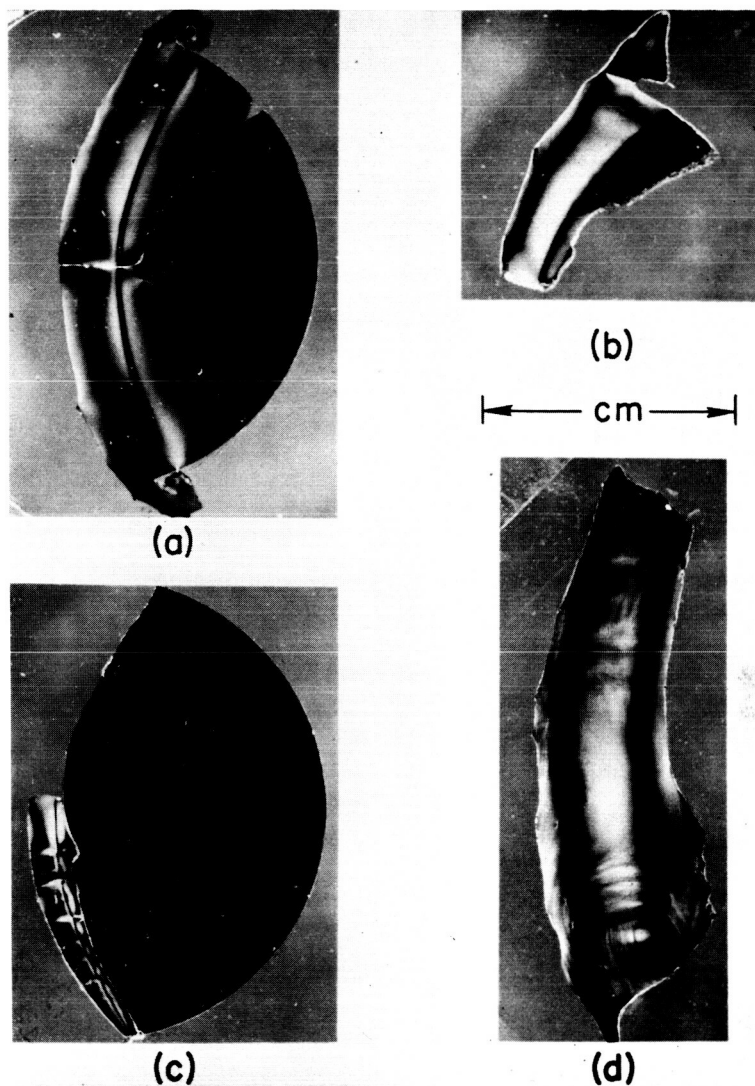Fig. 7. Fragments of aerothermal stress shell from Java.

Fig. 8. Thin sections in cross polarized light revealing stresses in aerothermal stress shell: (a) synthetic tektite glass model STG-2X; (b) australite fragment S.A.M. 743 from Nullarbor Plains; (c) synthetic tektite glass model STG-2V; (d) javanite fragment from Sangiran.
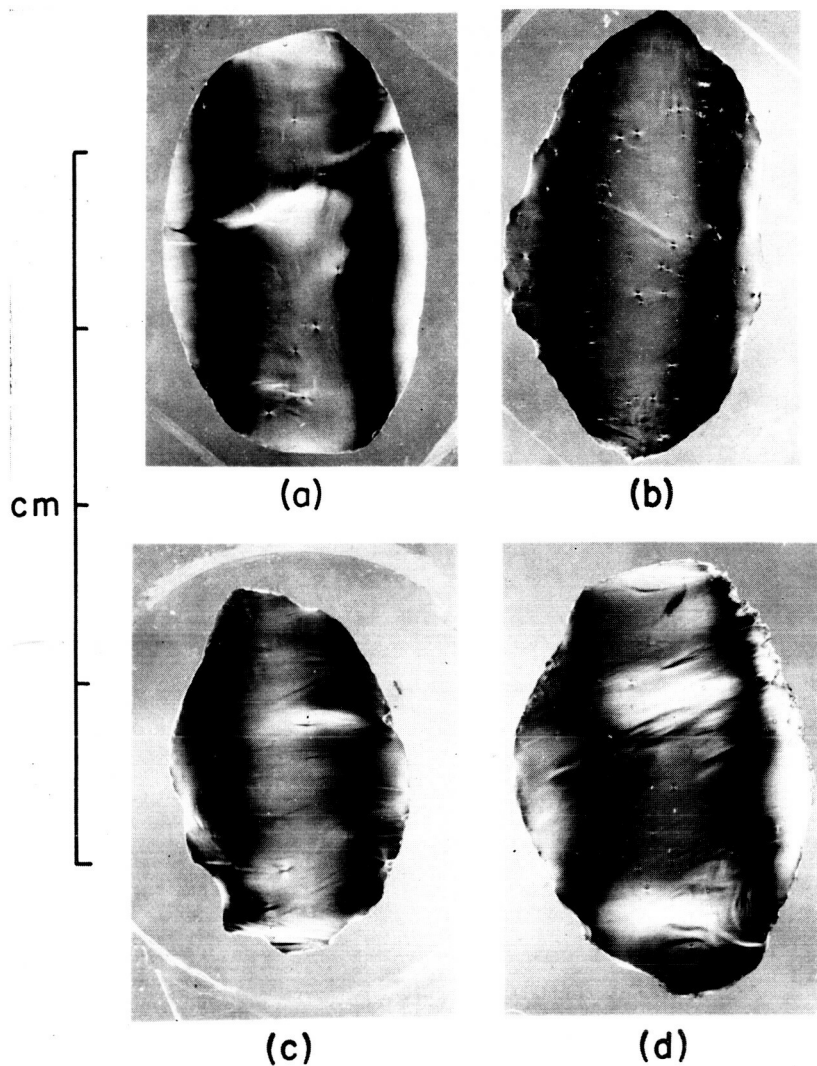
Fig. 9. Thin sections of Australasian tektite cores in cross polarized light: (a) australite AN22 probably from Mt. Davies Camp; (b) billitonite BN4; (c) philippinite U.S.N.M. 1910 from Santiago, Isabela; (d) philippinite U.S.N.M. 1906 from Santiago, Isabela.
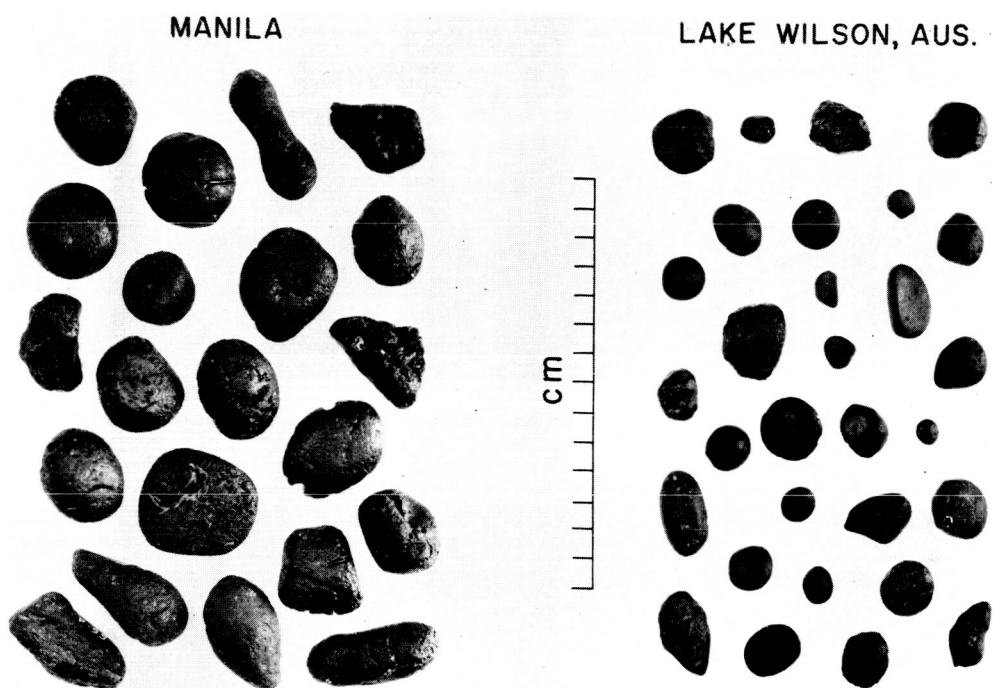
MANILA   LAKE WILSON, AUS.

cm

Fig. 10. Tektites from concentration centers.

cm

SOUTHEAST AUSTRALIA (VICTORIA)

SOUTHWEST WESTERN AUSTRALIA
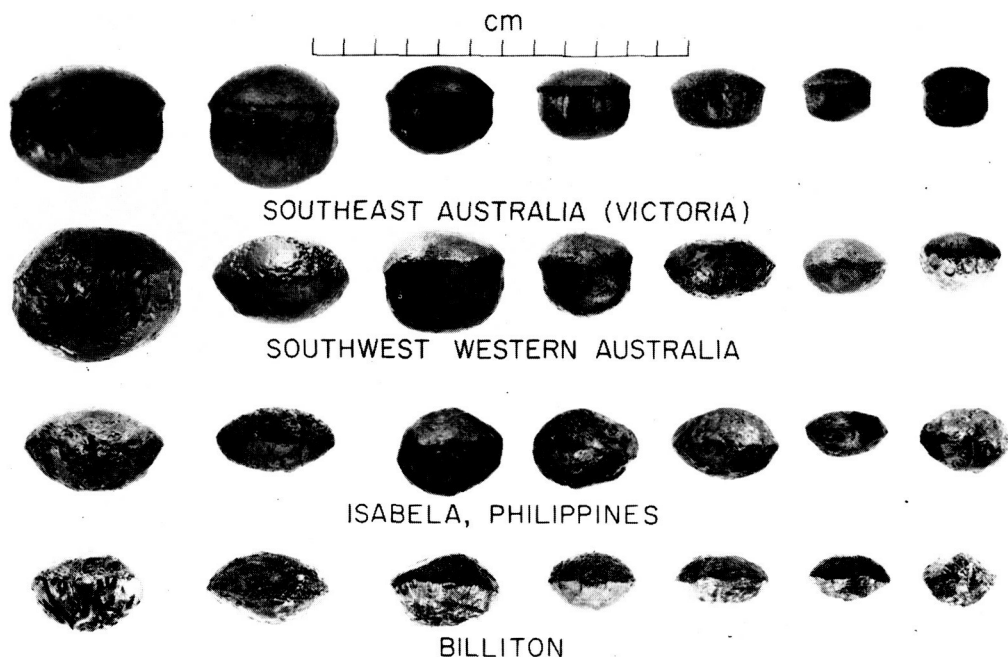
ISABELA, PHILIPPINES

BILLITON

Fig. 11. Side views of Australasian tektite cores.
(From left to right: Top row, N.M.V. E1986 Lake Wallace, N.M.V. 16869 Apsley,
N.M.V. E1955 Kanagulk, G.B. core Port Campbell, N.M.V. 5202 Mortlake,
N.M.V. 5211 Byaduk, G.B. 1070 Port Campbell, all localities in Victoria;
Second row, W.A.M. 3491 Corrigin, W.A.M. 10671 Bullaring, W.A.M. 10643
Mt. Barker, private collection from near Narembeen, W.A.M. 12123 near Mun-
tadgin, private collection from Kulin, W.A.M. 12074 near Woyaling, all localities
in southwest part of western Australia;
Third row, U.S.N.M.–1908,–1915,–1910,–1907,–1910,–2043,–1914, all from San-
tiago, Isabela;
Bottom row, N.A. BN-1, U.S.N.M. 77761, R.G.M. St20838, R.G.M. St9669b,
R.G.M. St20837, N.A. BN-4, R.G.M. St20974.)

concluded (1) that the centers of greatest tektite concentration virtually are useless insofar as concerns studies of aerodynamic evidence, or even studies of primary shapes, and (2) that there is a systematic progression, or continuity, in core sculpture across Australasia.

That the greatest concentrations of tektites have been brought about by terrestrial transportation, and are productive principally of thoroughly worn tektite pebbles, can be illustrated by the examples of Manila Bay and Lake Wilson. The australites from Lake Wilson are found in great abundance—one per square foot in some places (as noted in a memorandum of J. E. Johnson on file in the tektite collection of the South Australian Museum). The surface of this dry lake now serves as a repository for multitudes of australites that long ago were washed down along lines of water drainage from the slopes of the Mann Range nearby. Thus far the author has examined about 1800 specimens from Lake Wilson, a few of which are photographed in Fig. 10; none exhibit evidence of ring waves or flanges. A few core-like shapes are found, but with a well worn equatorial region in place of the sharp rim found in other areas where little transport has taken place. The processes of terrestrial transport which have concentrated the geographic distribution, have also obliterated the direct aerodynamic evidence of ring waves and flanges, as may be deduced from the resemblence of most Lake Wilson specimens to stream worn pebbles. A precisely similar situation exists in regard to the Philippine tektites found in extraordinary numbers around Manila Bay. Some examples from the Ortigas site, kindly presented to us by Mr. FRANCISCO ORTIGAS JR., are also illustrated in Fig. 10. Any record of aerodynamic evidence that once may have thinly covered the surfaces of these philippinites from Manila Bay has long since been replaced by a record of terrestrial wear and etching. It is evident that in making observations of the variations in core sculpturing and in primary shapes across Australasia, localities such as Lake Wilson and Manila Bay can yield little information. In the Philippines the tektites found at Isabela are less worn and are employed herein for such observations.

That there is a systematic variation across Australasia in the types of primary core shapes is illustrated by the photographs in Fig. 11. Here the side views of 28 different tektites are presented, each of which represents a tektite core that is either round in plan form or nearly round. They are arranged in four rows of seven tektites each, with cores from Victoria, southeast Australia, in the top row; cores from the extreme southwest of Australia in the second row; cores from Isabela, Philippines, in the third row; and cores from Billiton Island in the bottom row. All cores are oriented in the attitude corresponding to flight vertically downward with the base at the top, and the surface from which the aerothermal stress layer spalled at the bottom. The cores from southeast Australia invariably exhibit a smoothly curved base, forming a segment of a sphere in many cases. Such regular shapes are indicative of primary formation at a relatively high temperature, where the glass viscosity was sufficiently low for the weak forces of surface tension to contract any surface irregularities into smoothly round contours prior to solidification. In the second row it is seen that, in contrast, the majority of these cores does not exhibit a smoothly curved base. Localities for this second row encompass a region within about 200 kilometers from Kulin in the southwest portion of western Australia. In this area, about two-thirds of the cores

exhibit a base surface that is irregularly contoured, often somewhat faceted in shape. But smoothly and irregularly shaped bases alike are truncated by a sharp circumferential rim. Thus little abrasion has taken place on these particular specimens and the irregular contours of the base surface are not to be attributed to processes of terrestrial abrasion. It is concluded that the primary tektite shapes in southwest Australia commonly were rather irregular, in contrast to the nearly perfect figures of revolution prevalent in southeast Australia. Since the average density is higher in the southwest, the silica content is lower, and the viscosity would be lower for a given temperature of formation; this should promote rather than retard the formation of smoothly curved primary shapes. Consequently, it follows that the temperature of formation of tektites in southwest Australia was lower than that in southeast Australia.

Cores with irregularly curved bases are even more prevalent in the Philippines and Billiton than in southwest Australia. Among about 200 billitonites examined, only two (U.S.N.M. 77761 and R.G.M. St9669b, second and fourth from left, respectively, in the fourth row of Fig. 11) exhibited smoothly curved bases; and among several thousand philippinites from Isabela, only one such was observed (U.S.N.M. 1915, second from left in the third row). On this basis a qualitative ordering of the temperatures of formation has been arrived at, with the highest temperature in southeast Australia and progressively lower temperatures in southwest Australia, then Billiton and finally the Philippines. The continuity in core sculpture across Australasia is evident from the examples of Fig. 11.

It also may be seen in Fig. 11 that the core sculpturing in the southwest part of western Australia more closely resembles that in the Philippines than that in southeast Australia. Compare, for example, the lens-like cores second from left in rows 2 and 3, and note the close similarity of the three southwest australite cores in the right portion of row 2 with the three philippinite cores just beneath them. It is noted that several navels unmistakably are exhibited on australite W.A.M. 12074, situated at the extreme right in row 2. Such navels are common on philippinites and billitonites, and this situation is parallel to that previously described in relation to the worm grooves. The similarity in core sculpture observed between tektites from the Philippines and southwest Australia is to be viewed in the light of previous evidence of coincident chemistry and of coincident population polygons between these same two regions; these two widely separated groups of tektites obviously are from separate portions of one and the same cluster.

The qualitative deductions outlined above, of a progressively lower temperature of formation from the southeast to the northern portions of the australasian strewnfield, have been substantiated by independent laboratory experiments which enable the deductions to be placed on an approximate quantitative basis. In the far north west of the strewnfield the dominant shapes are teardrops and other severely stretched forms. Such shapes result when a molten glass mass of very high viscosity is disrupted into many component blobs as it cools. As part of our program of research on tektites, experiments have been preformed in which a mass of molten glass was heated to different temperatures and ejected into the atmosphere at different velocities. These experiments were conducted by my colleague, Mr. George Lee. In one experiment glass was ejected into the air at a sufficiently low velocity

(several m/sec) that the disruption was dominated by surface tension forces rather than aerodynamic pressure forces. The glass was ejected out of a tube from a vantage point sufficiently high (34 m) that the forms solidified prior to striking the ground. When the glass viscosity was 2·8 P, the distribution of forms produced was similar to the distribution of primary australite shapes in southeast Australia (CHAPMAN and LARSON, 1963). When the glass viscosity was 35 P, however, mostly teardrops were produced, and when reduced to 0·8 P, almost all spheres were produced. These circumstances are illustrated in Fig. 12. It is clear that the viscosity of the fused parent material producing the southeast Asian teardrops was much higher than that producing the Victorian australite round forms; the corresponding temperature, however, would have been only slightly lower. Thus, for a viscosity of 35 P, the temperature would be about 2100°C, whereas for a viscosity of 2·8 P it would be about 2600°C. These rough estimates of the temperatures of formations of indochinites and australites, respectively, appear quite reasonable. This indicated trend of lower formation temperatures for the northern portion of Australasia agrees with the trend deduced above from observations of the progressive variations in core shapes across the strewnfield.

In summary, thus far, it has been shown that the formation and spontaneous spallation of an aerothermal stress shell is responsible for the characteristic sculpture of Australasian tektite cores. Thus, billitonites and philippinites, as well as australites and javanites, alike have descended into the Earth's atmosphere as rigid glass objects and have been sculptured by aerodynamic ablation. The angle of entry was steeper in Java than in Australia. The progressive change in core shape from Australia to the Philippines is compatible with the change from dominantly round forms in southeast Australia to dominantly teardrop shapes in southeast Asia; both changes indicate that the temperature of formation was highest for the tektites that fell in southeast Australia and lowest for those that fell to the north in the Philippines and southeast Asia. These circumstances of tektite unity across Australasia, combined with the observation of chemical identity between tektites from southwest Australia and the Philippines—the same two areas which exhibit essentially congruent population polygons—constitute firm evidence that all the Australasian tektites originated in a single event.

PART II. ATMOSPHERE ENTRY TRAJECTORIES AND ORIGIN

In view of the compelling evidence that a single impact produced all of the Australasian tektites, a determination of the origin of any portion would provide the origin of all. It is fortunate that the australites which fell in southeast Australia were simple figures of revolution including many spheres, because such shapes are amenable to quantitative aerodynamic analysis. Ablation in hypervelocity flight transformed these simple primary shapes into secondary shapes which today exhibit an aerodynamic record that is sufficiently complete to determine their entry trajectory and, hence, place of origin. Originally, two sources of aerodynamic evidence were employed for trajectory determination: the amount of ablation at the stagnation point, and the systematic distortions of internal striae within a thin layer just beneath the front face (CHAPMAN, 1960). Subsequently, a third source of evidence

was developed, namely, that given by the spacing between ring waves on the front face (CHAPMAN and LARSON, 1963). In this part of the paper the previous aerodynamic evidence is supplemented in three ways: (i) the ring-wave evidence is sharpened through experiments in which the effect of variable body forces on ring-wave spacing is evaluated; (ii) the ablation evidence is refined through observations which remove any uncertainty about pre-entry turning; and (iii) a new source of evidence is tapped from experiments in which a relationship between deceleration in flight and flange shape is established.
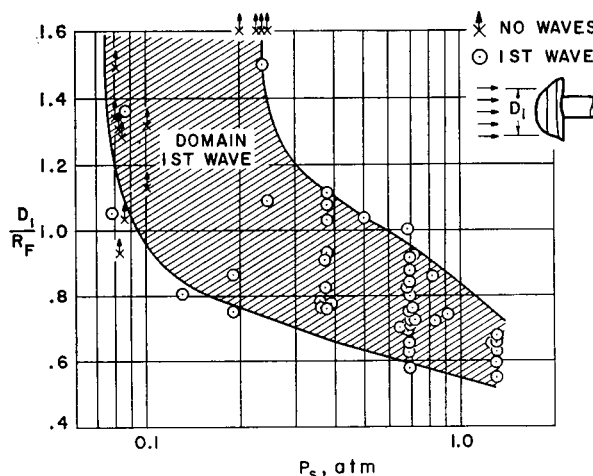

Fig. 13. First ring wave diameter from aerodynamic ablation experiments on tektite glass.

ATMOSPHERE-ENTRY EVIDENCE PROVIDED BY RING-WAVE SPACING

The results of experiments on the aerodynamic ablation of tektite glass (*ibid.*, pp. 4329–4331) have shown that the principal variable affecting the spacing between ring waves is the stagnation-point pressure p_s. Such circumstances are analogous to the behavior of waves produced by wind over water: the stronger the wind, the more prevalent are the waves. In a hypervelocity entry, or in a laboratory experiment, the "wind" over the front face will be determined mainly by the stagnation pressure. Experimental data from ablation experiments with tektite glass are presented in Fig. 13, and clearly show that the first wave forms at a smaller diameter as p_s increases. The data are plotted in terms of the ratio of first wave diameter D_1 to front surface radius of curvature R_F. It is to be noted that these data were obtained under test conditions which match the actual velocity and air density that exist in flight at the termination of ablation, as well as the actual size and material composition of australite buttons. The only flight parameter not matched is the ratio of body forces F_B (deceleration force in flight, gravitational force in the wind tunnel) to aerodynamic forces F_A; and a special experimental investigation has been conducted to evaluate the dependence of D_1/R_F on F_B/F_A. Details of this investigation are relegated to Appendix A, since some aerodynamic considerations are involved that may be as uninteresting as they are unfamiliar to most readers of this journal. It will
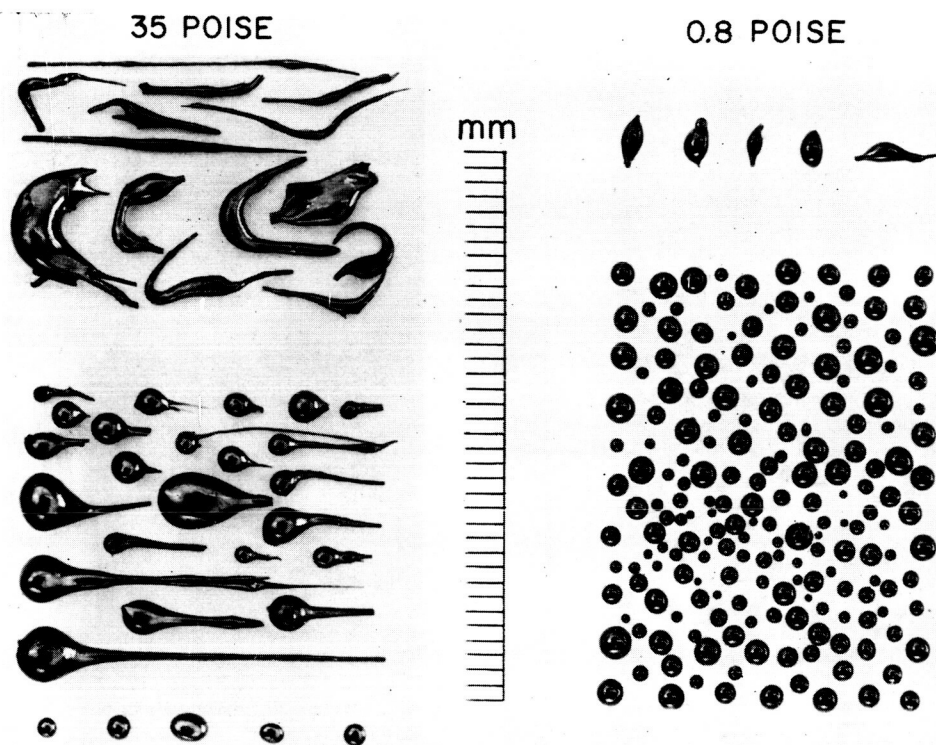
35 POISE 0.8 POISE

mm

Fig. 12. Dependence of primary form on glass viscosity at breakup.

AERODYNAMIC ABLATION AUSTRALITES

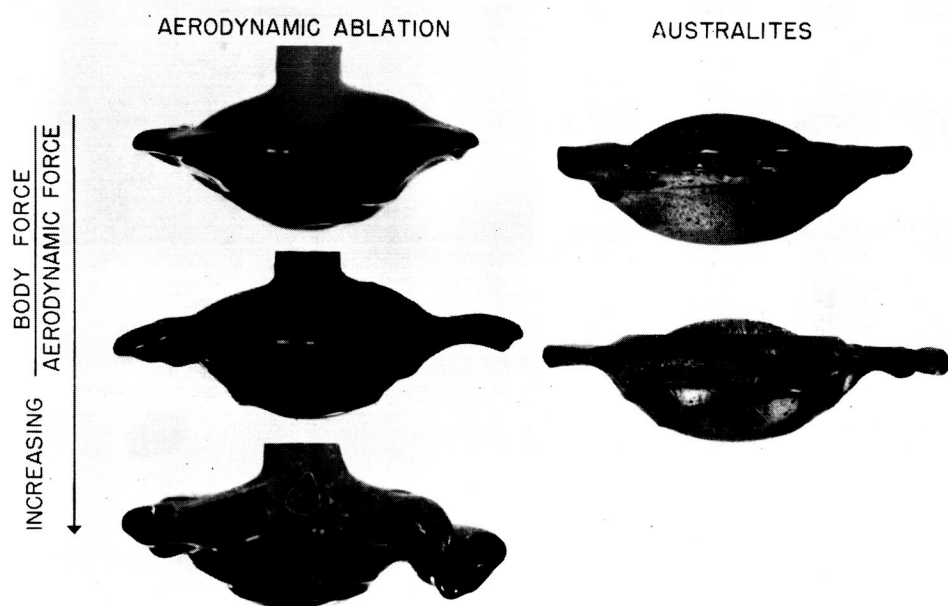BODY FORCE / AERODYNAMIC FORCE

INCREASING

Fig. 14. Ablation of glycerin glass under varying ratio of body force to aero-
dynamic force, and comparison with australites (S.A.M. 625 top right and
U.M.G.D. 2575 beneath).

Fig. 17. Australites not aerodynamically oriented at termination of ablation (top row S.A.M. 956 from central Australia; center row S.A.M. 1181 from Kingscote, South Australia; bottom row S.A.M. 443 from Kalgoorlie area).
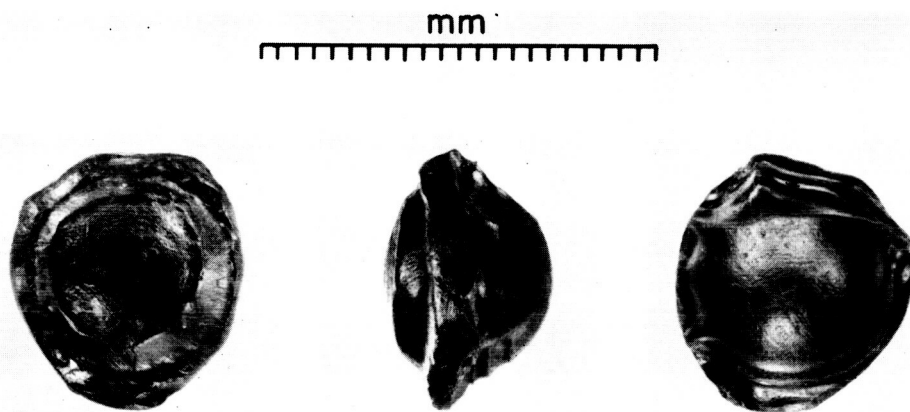

Fig. 18. Three views of australite with ring waves on both sides (S.A.M. 431; Kalgoorlie area).

g's FOR
TEKTITE
GLASS

7

21

49

140

280

AUSTRALITE

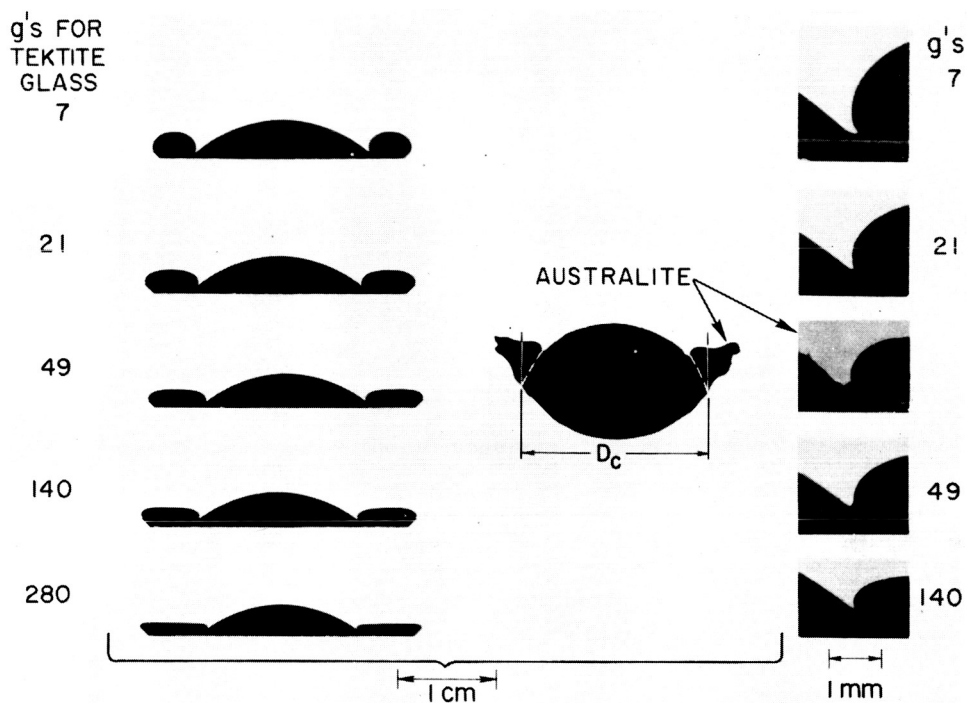D_c

g's

7

21

49

140

1 cm

1 mm

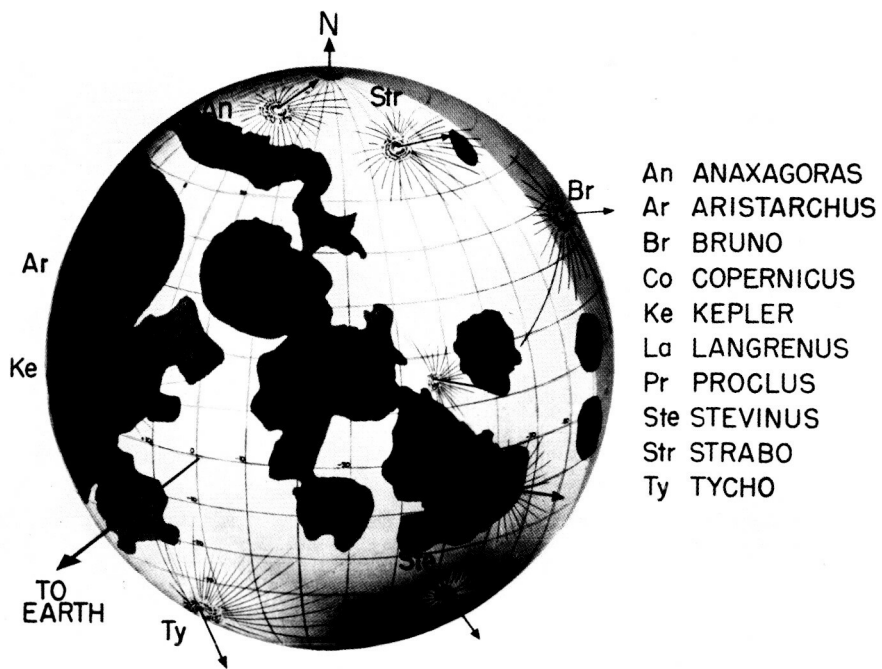Fig. 19. Flange flattening with increasing deceleration.

Fig. 23. Ten rayed craters investigated.

suffice here to mention that, from laboratory ablation experiments in which mechanical similarity with australite flight conditions has been achieved (Fig. 14), the effect of body forces in the most extreme case—namely, that in which a wide hat-brim-like flange is formed—has been shown to be equivalent to a reduction in stagnation pressure by a factor of about two (Fig. 15). The theoretical foundation for expressing the effect of body forces in terms of an equivalent factor in p_s is outlined in Appendix A.
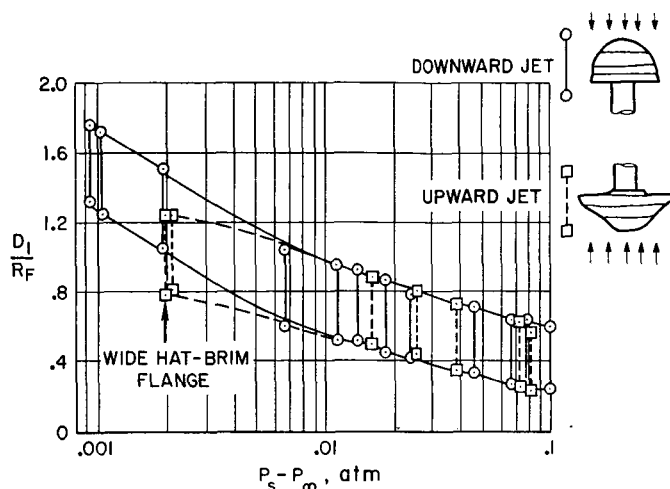

Fig. 15. Effect of body forces on diameter of first ring wave; glycerin glass.

At first it might appear surprising that the decelerational body force in flight does not exert a greater influence on the ring-wave spacing. These circumstances become more understandable when it is realised that the deceleration is, in fact, produced by, and is directly proportional to, the stagnation pressure; and that the velocity ring-wave propagation along the melt layer is an order of magnitude greater than the velocity of the flowing glass layer. In the region of the stagnation point where the first wave forms, the experiments with glycerine glass ablation showed the ring-wave velocity at any given distance x from the stagnation point to be between about 7 and 10 times the computed surface velocity u_w of the receding glass layer. Since $u(y)$ is nearly an exponential function and $u(o) = u_w$, this means that the ring-wave propagation velocity is greater than the mean velocity in the liquid layer by about a factor of between 20 and 28. Under such circumstances it is pictured that the driving forces of the external wind in combination with the viscosity and thickness of the liquid layer are the major variables determining ring-wave spacing, and that the perturbations by body forces of these relatively slow movements of this liquid layer are not of major consequence to the relatively fast motion of the wave.

With the effects of body forces on ring-wave diameter evaluated, the experimental data of Fig. 13 can be used to determine both an upper and lower limit on the stagnation pressure which existed at the termination of ablation in flight. For such a determination it is necessary to know the range of D_1/R_F values encountered in flight. Numerous measurements of D_1/R_F have been made on australites from the

southwest Victoria area. The results are presented in Fig. 16 plotted as a function of the amount of ablation y_s determined in a manner described subsequently. At one extreme of the data is a high ablation group (y_s about 1·2 cm) corresponding to a ring-wave range $0.7 < D_1/R_F < 1.2$ whereas at the other extreme is a low-ablation group (y_s about 0·5 to 0·6 cm) corresponding to $0.6 < D_1/R_F < 1.0$. The D_1/R_F range for the high-ablation portion would correspond to $p_{s_f} = 0.3$ atm in the absence of significant body forces (Fig. 13); but the effect of decelerational body forces in
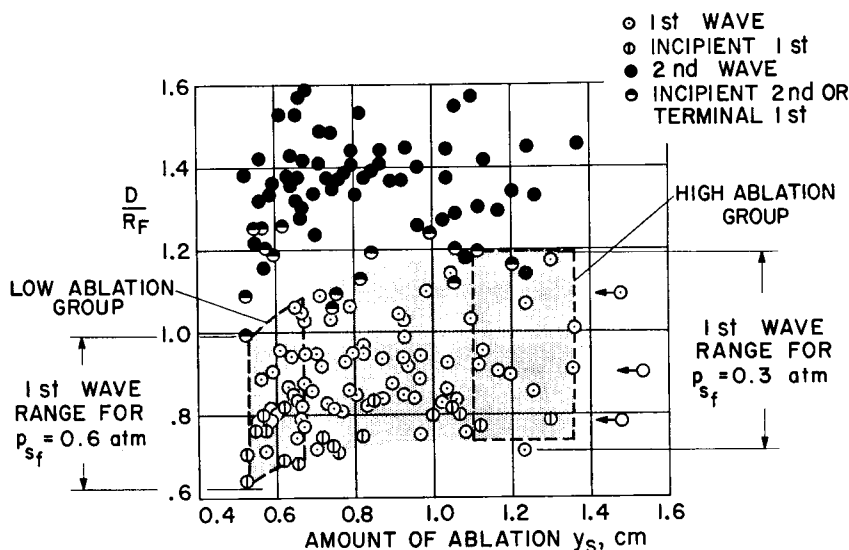

Fig. 16. Variation of ring wave diameter with amount of ablation; Victoria australites.

flight is to reduce D_1 somewhat, and therefore $p_{s_f} = 0.3$ atm would be an upper limit on the pressure which existed in flight when ablation terminated on this group. Since the effect of body forces on tektites corresponds to less than a factor of 2·0 in pressure variation, the value $p_s = 0.15$ atm would be a lower limit on the stagnation pressure for this same high-ablation portion. The D_1/R_F range for the low-ablation portion, on the other hand, corresponds to $p_{s_f} = 0.6$ atm as an upper limit and 0·3 atm as a lower limit. On the southwest Victoria australites, the experimental evidence pertinent to trajectory determination from observations of ring-wave spacing shows, therefore, that (1) all trajectories correspond to $p_{s_f} < 0.6$ atm, and (2) that the high-ablation portion corresponds to $0.15 < p_{s_f} < 0.3$ atm and the low-ablation portion to $0.3 < p_{s_f} < 0.6$. These conditions on p_{s_f} are readily converted into limiting conditions on the initial velocity V_i and angle γ_i of entry into the atmosphere, as will be seen subsequently.

ATMOSPHERE-ENTRY EVIDENCE PROVIDED BY AUSTRALITE GEOMETRY

The most important aerodynamic quantity determined from study of australite geometry is the amount of ablation that has taken place at the stagnation point. Knowledge of this quantity enables certain conditions about the entry trajectory to be computed provided that the shape is a round form, and that during entry it

remained in a fixed orientation with its axis of symmetry parallel to the flight path. Two complications are involved here: (1) prior to entry, not all round form australites were spheres, the only shape for which the amount of ablation readily can be deduced; and (2) prior to entry some of the australites were turning. The first of these complications has been circumvented (CHAPMAN and LARSON, 1963) by measuring—with dial-indicator curvature gages and circular-arc templates—the variation in curvature over the base of numerous round-form australites, and then compiling data for trajectory analysis only on those specimens which exhibit essentially constant curvature over the base and which therefore were nearly spherical prior to entry. The second complication has been circumvented by compiling enough data corresponding to a given australite area to enable a selection to be made of those specimens which either were turning about an axis parallel to the flight path, or were not turning at all and whose ablation would be the same as that for fixed orientation flight. The procedure and reasoning underlying such a selection are outlined in this section.

Although most of the australites possessed an essentially fixed orientation at the time ablation terminated, there is decisive evidence that some tumbled, some wobbled, and some flopped during ablative flight. This means that many australites probably were slowly turning prior to entry. Australites commonly exhibit beautifully symmetric patterns of ring waves on their front, and show no superficial melt patterns on their base, thus bearing mute evidence that aerodynamic stability in most cases had been achieved by the time ablation terminated in flight. In contradistinction, a very small percentage exhibits an irregularly meshed pattern of waves over most of their surface, and superficial melt patterns elsewhere, thus revealing equally certain evidence that they were still tumbling or wobbling when ablation terminated. Three illustrative examples of the latter are presented in Fig. 17, where three views of each specimen are shown. The specimen photographed in the top row (S.A.M. 956 from central Australia) is covered over its entire surface with an irregular mesh of flow ridges. Its slight flange provides an indication of its orientation when ablation terminated. This specimen evidently tumbled throughout the ablative phase of its entry. A sufficient rate of pre-entry rotation about an axis inclined to the flight path would produce such a configuration. The broken dumbell in the second row (S.A.M. 1181 from Kingscote, south Australia) and the complete elongate specimen in the bottom row (S.A.M. 443 from the Kalgoorlie district) provide good examples of pre-entry turning which was almost, but not quite, damped out when ablation stopped. These two specimens exhibit the irregularly meshed pattern of flow ridges mainly on one side, the opposite side of which reveals the contour of the primary shape marred in a few places by spots of melting, but otherwise indicative of the shape before entry.

In addition to the evidence of tumbling or wobbling, as revealed by patterns of irregular meshed flow waves, evidence of some other type of turning in flight also is revealed by an unusual type of flow wave pattern that has been observed. Three views of an australite with ring waves and other flow ridges clearly exhibited on both sides are presented in Fig. 18. The wave patterns on each side of this tektite are surprisingly regular, indicating that both sides faced forward at different times in flight, possibly as a result of a rather sudden flopping at some stage during entry.

If a tektite turns during entry the maximum depth of ablation is greatly reduced. From measurements of the base curvature on the two elongate specimens of Fig. 17, the maximum amount of ablation of the front face turns out to be only $y_s = 0.28$ cm for S.A.M. 1181, and 0.21 cm for S.A.M. 443. On other specimens examined, it is only 0.1 cm, but usually is about 0.2 cm for elongate specimens that were not oriented in flight. Depths of ablation of this magnitude are very much less than on most buttons (1 cm average for y_s) because turning distributes the locally severe stagnation-point heating all around the specimen. Only a small part of this difference in ablation (between 0.2 and 1 cm) is due to the inherent difference between ablation of an elongate and of a sphere, since stagnation-point heating is only 30 per cent less on an elongate than on a sphere. The major part of the difference is attributed to the fact that, as an object turns about an axis transverse to the flight path, the average heating rate at any point on the body would be only about one-fourth that at a stagnation point; moreover, the average pressure gradient is not always directed in a manner which would consistently remove melted glass, as it is in the case of a fixed orientation, but instead is reversed intermittently at each turning; also, the average pressure at any point during turning is much less than the stagnation pressure. Thus these circumstances combine to produce only 2 mm of ablation on a turning tektite, in contrast to 1 cm on one not turning. Consequently, unless careful attention is paid to this problem, considerable error can be introduced into a determination of the entry trajectory from a given amount of ablation. In the investigations of ADAMS (1963) and O'KEEFE (1963) the complication of pre-entry turning in affecting the amount of ablation has been overlooked.

It is possible to select from a sufficiently large sample of tektites on which appropriate measurements have been made, a certain portion for trajectory analysis that is free from uncertainties about pre-entry turning. The appropriate measurements on one such sample from Victoria already have been presented (Fig. 16). Prior to entry, either (a) none of these primary australite spheres were turning in a fashion affecting ablation, or (b) at least some were turning in such a fashion. If (a) is the case, then any specimen of the total sample can be analysed for its entry trajectory, and, in particular, the high-ablation portion (y_s about 1.2 cm) would comprise a valid group for trajectory analysis (so also would the low-ablation portion in this event). If (b) is the case, then those which were turning transverse to the flight axis would ablate less, and the high-ablation portion would represent those turning parallel to the flight axis combined with those not turning. Since turning parallel to the flight path does not have any appreciable effect on the amount of ablation, it follows that in either event (a) or (b) the high-ablation portion represents a valid group for which the entry trajectories can be computed free from uncertainty about pre-entry turning. The low-ablation portion would give only a lower limit on the amount of ablation if (b) is the case. Before presenting results of trajectory determinations for both of these groups, however, a brief account will be given of some new experimental evidence pertaining to the entry trajectories of australite buttons.

ATMOSPHERE-ENTRY EVIDENCE PROVIDED BY FLANGE SHAPE

The deceleration forces encountered in flight have a major effect in determining the flange shape: the greater the deceleration the flatter the flange. These forces

are opposed by surface tension forces which tend to round the flanges. Surface tension of tektite glass is sufficiently high (390 dyn/cm, as measured from sessile drop experiments at the Ames Research Center by Mr. Frank Centolanzi) that a drop at 1 g readily stands 6 mm above its supporting surface. Since flanges before solidification were toroidal drops of tektite glass flattened to the order of 1 mm equivalent height, it follows that the tektites were experiencing much more than 1 g deceleration *when the flange solidified*, and that the flatness of the flange gives a measure of this deceleration.

In order to obtain quantitative values for the decelerations encountered by australite buttons—and thereby obtain new quantitative information on the velocity and angle of entry into the atmosphere—some experiments pertaining to flange shape have been conducted in a centrifuge. Since a full description of these experiments, which have been performed by my colleague, Mr. Norman Zimmerman, would swell the several paragraphs which follow into the proportions of a separate paper, only a brief account is given here.

The experimental technique that has been developed is rather novel, and requires some explanation. A ring of mercury first is poured around the circumference of a spherical segment of metal resting with its base on the bottom of a centrifuge bucket. A mixture of silicone rubber and catalyst is poured into the bucket, and the centrifuge then spun at a constant number of g's until the rubber has set. From the rubber mold a cast is made and meridionally sectioned to reveal the combined profile of the spherical segment with its surrounding toroidal flange. A quantitative evaluation of the data obtained requires knowledge of the surface tension of mercury immersed in silicone rubber, and this is determined experimentally by the sessile drop method. The mercury flanges were of the same dimensions as those on typical australites so that a mercury profile formed at some particular deceleration value G_{Hg} would correspond to a tektite-glass profile formed at a value G_T equal to $G_{Hg}(\rho_{Hg}\tau/\rho\tau_{Hg})$, where τ_{Hg} and ρ_{Hg} designate, respectively, the surface tension and density difference of mercury in silicone rubber, while τ and ρ designate the corresponding quantities for tektite glass in air. The net result is $G_T = 7G_{Hg}$.

Some flange profiles from the centrifuge experiments are compared in Fig. 19 with the profile of an australite button. At the left are photographs of five meridional sections which illustrate the progressive flattening of the flange as the body force in the centrifuge is increased from 7 to 280 g's. These g-values would correspond to the deceleration of tektite glass in flight. By extrapolation of the trend exhibited in these examples, a tektite-flange profile for 1 g would be expected to be essentially circular; and this is indeed observed in our ablation experiments with tektite glass. The physical conditions in the centrifuge experiments differ from those in flight in one important respect. In flight a supporting base for the flange melt exists only inboard of the diameter D_c of the lens-shaped core. Outboard of this diameter the flange can be bent either upward or downward depending on the relative magnitude of the aerodynamic and deceleration forces in this outer region. The portion of flange inboard of D_c, and especially in the immediate region of the inner diameter of the flange, is not significantly affected by aerodynamic forces since these are very small in the low-pressure region behind the base, and since the solid core provides protection from the aerodynamic forces on the front face. Consequently, only the inner

portion of an australite flange can be compared with the centrifuge experiments. At the right in Fig. 19 a close up of this region for an australite button (G.M.M. 8355 from Uralla) is compared with the corresponding close-ups from the centrifuge experiment. It is evident that the degree of flange flattening on this australite is only slightly less than the experimental profile for 49 g's, and would be equivalent to about 45 g in flight. Flanges on australites from Victoria correspond to a somewhat smaller value of about 30 g, which is used subsequently in determining one limit on the trajectories of the high-ablation portion of Victorian australites.

It is important to observe that the number of g's deduced from a comparison of tektite flange and centrifuge model corresponds to the deceleration which existed when the flange solidified in flight. As long as ablation is proceeding, the flange continually is formed from fresh melt and is flattened to whatever degree is appropriate for the temporarily varying value of deceleration G. During an entry, G first increases as the tektite descends into increasingly dense layers of air, then reaches a peak, and finally decreases when the velocity has been substantially reduced by the drag forces. In the velocity range of interest, tektite glass does not stop ablating until the peak deceleration is passed; and the flange does not solidify until sometime after ablation stops, since it takes a finite time for the flange to cool to rigidity. Thus the final flange shape is formed when the deceleration is considerably less than the deceleration G_f which existed at the instant when ablation terminated. Therefore, by comparing australite flanges with centrifuge experiments and deducing therefrom some value for G_f we obtain a firm *lower* limit on G_f. The actual value of G_f would be considerably higher than the lower limit so deduced.

COMBINATION OF EVIDENCE TO DEDUCE ENTRY TRAJECTORIES AND TEKTITE ORIGIN

Computations have been made of the range of initial entry velocity V_i and entry angle γ_i compatible with the observed amount of ablation on the high-ablation group of Victoria australites. The pertinent physical properties of tektite glass have been measured,* and the ablation characteristics as calculated by two independent methods have been shown to agree with laboratory experiments (CHAPMAN and LARSON, 1963) within a variation of about ± 10 per cent in the amount of ablation. Such a variation is equivalent to that represented by the high-ablation group $y_s = 1 \cdot 1$–$1 \cdot 3$ cm. Results of the computations are presented in Fig. 20(a) where the shaded regions designate areas in the $V_i(\gamma_i)$ plot which are excluded as being incompatible with the observed amount of ablation. Thus, below about 5 km/sec entry velocity there would be no ablation; below and to the right of the open corridor there would be too little ablation; while above and to the left there would be too much ablation. It is noted that the lower boundary corresponds to the lower range ($y_i = 1 \cdot 1$ cm) of the high-ablation group as computed by a method (designated II, *ibid.*) which tends to yield slightly low velocities, whereas the upper boundary

---

* At the Second International Tektite Symposium some measurements purported to represent vapor pressure of tektite glass were presented by L. Walter. His values for p_v are several orders of magnitude different than the values used herein. Accordingly, a brief account of various ablation experiments establishing the accuracy of the values used herein is presented in Appendix B to this paper. It is shown there that the use of Walter's values would result in very large errors in ablation calculations.

corresponds to the upper range ($y_s = 1.3$ cm) of this group as computed by a method (designated I) which tends to yield slightly high velocities. Consequently, for any given entry angle the corridor so delineated provides both upper and lower limits on the entry trajectories of these Victoria australites.

In computing the amount of ablation it has been assumed that the australite primary spheres were cool prior to entry into the atmosphere. It is important to recognize that variations in the initial temperature do not significantly affect
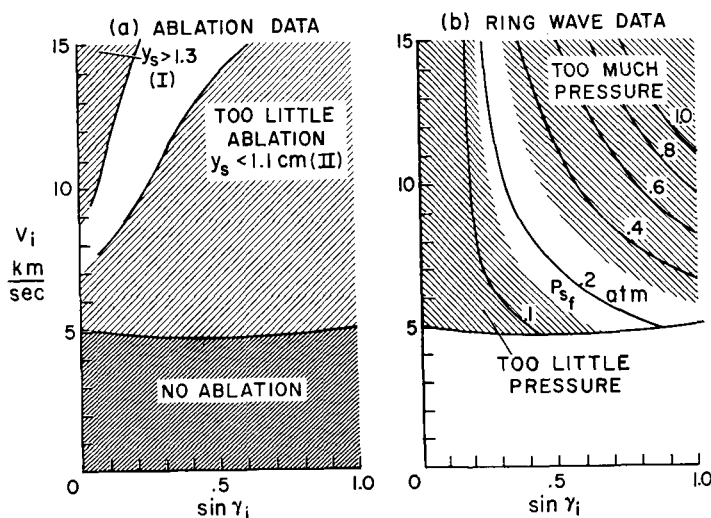

Fig. 20. Entry conditions for high-ablation group of Victoria australites as determined from ablation and ring-wave data.

ablation as long as the glass is cool enough to be rigid. Many large australite cores have a spherical-segment after-body which, from considerations of aerodynamic stability, could not be the result of deformation by the aerodynamic forces to which they were subjected. Such cores, therefore, were not soft, but were rigid prior to entry; and their initial temperature T_i definitely was less than about 1200°K, the softening temperature under the deceleration conditions of flight. Actually, T_i must have been considerably less than about 920°K, the strain temperature, in order to have produced spallation-prone tensile stresses only within a thin shell under the front face of these cores. That the amount of ablation is not significantly affected by variations in T_i in the range below the strain temperature, is illustrated by the following calculations (for $\gamma_i = 45°$, $V_i = 11$ km/sec, $R_0 = 1.5$ cm, and $P_v = P_v$ ($\dot{m}$) Appendix B)).

Initial temperature T_i, °K	Amount of ablation y_s, cm
300	0.60
600	0.65
900	0.71
1200	1.82

Since the buttons analysed herein are smaller than the cores, they would have been even cooler upon entry, and certainly cool enough that a knowledge of their exact initial temperature is unimportant to the determination of entry trajectories from the observed amount of ablation.

Ablation data alone do not determine an entry trajectory. As is evident from Fig. 20(a), the entry velocity may be as low as 8 km/sec if the flight path is essentially horizontal (sin $\gamma_i = 0$), or greater than 20 km/sec if it is vertical (sin $\gamma_i = 1$), and
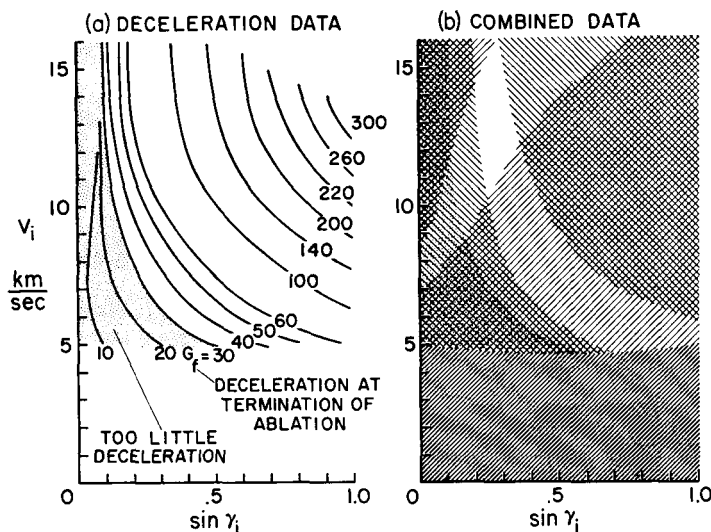

Fig. 21. Entry conditions for high-ablation group of Victoria australites as determined from deceleration and combined data.

still be compatible with the observed amount of ablation. Some additional and independent type of observational data are required to determine the entry angle. The observational data and laboratory experiments on ring-wave diameter provide one such source of data: the pressure p_{s_f} at the end of ablation was between 0·15 and 0·3 atm for the high-ablation group. Shown on the $V_i(\gamma_i)$ in Fig. 20(b) are the lines of constant p_{s_f} (for $R_B = 1$ cm), from which the boundaries have been determined of the areas representing both too much pressure and too little pressure to be compatible with the observational data. (The value of p_{s_f} is proportional to the base radius within the narrow R_B range of 0·8 to 1·2 cm covered by the particular australites investigated.)

A lower limit on the deceleration G_f which existed at the termination of ablation, as noted earlier, is about 30 g for the Victoria australites; and the $V_i(\gamma_i)$ area excluded by this limit is shown shaded in Fig. 21(a). The $V_i(\gamma_i)$ point corresponding to the entry trajectory may be anywhere in the region to the right and above the $G_f = 30$ g boundary. In essence, therefore, the deceleration evidence shows that the australites have not entered at very shallow angles, but this evidence does not show how steep the entry angle might have been.

A determination of both the entry velocity and angle is achieved by superimposing on one $V_i(\gamma_i)$ plot the various shaded areas excluded by the combined aerodynamic

evidence. Such a plot, shown in Fig. 21(b) for the high-ablation group, yields a diamond-shaped domain: trajectories within this domain bounded by $10 < V_i$ (km/sec) < 16 and $0.2 < \sin < 0.4$ (corresponding to $12° < \gamma_i < 25°$) would be compatible with the observational data on amount of ablation, ring-wave diameter, and flange flattening. Any point exterior to this domain would correspond to a trajectory that is incompatible with one or more of the three types of evidence for the high-ablation group of Victoria australites.
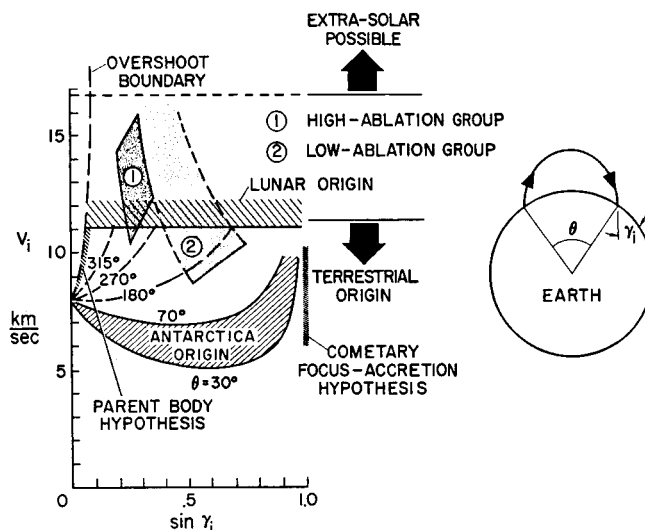

Fig. 22. Comparison of aerodynamic trajectory evidence for Victoria australites with various hypotheses of tektite origin.

Knowledge of an australite entry trajectory determines the place of origin of the Australasian tektites, for it is a simple matter to trace an entry trajectory backwards. The significance of this aerodynamic evidence is attested by the number of hypotheses of tektite origin which are excluded by it. In the past a magnificent variety of hypotheses have been advanced by scientists who were either unfamiliar with or unaware of the modern developments of atmosphere entry physics; and to this date new theories are still being casually suggested, and old ones tenaciously promulgated that manifestly are incompatible with aerodynamic evidence that has been established by flight and laboratory experiments. It is of significance, then, to illustrate why the aerodynamic evidence excludes hypotheses of origin which require either that the entry be too fast (extrasolar origin), too slow (Antarctica origin or origin from any nearby continent), too shallow (parent body hypothesis,) or too steep (cometary focus–accretion hypothesis). A $V_i(\gamma_i)$ plot is presented in Fig. 22 on which the domains of various hypotheses are shown in comparison to the domains delineated by the over-all aerodynamic evidence. Computations for the low-ablation group of Victoria australites also are included on this plot. Because of the effects of pre-entry turning, however, an upper limit on velocity cannot accurately be fixed for this group. Consequently, instead of showing an upper-left boundary line for the low-ablation group, its domain is terminated by a gradual diminution in shading as a

8

reminder of these circumstances. From Fig. 22 it is evident that the aerodynamic evidence provides no support, and, in fact, contradicts: (1) an extrasolar origin (KOHMAN, 1958) since the required entry velocities are too high (greater than 16·7 km/sec); (2) the parent body ablation-drop hypothesis (HARDCASTLE, 1926; O'KEEFE 1963; ADAMS, 1963), since the required entry conditions are in a thin strip adjacent to the overshoot boundary at entry angles much too shallow to be compatible with either the observed ring-wave spacing (especially on the low-ablation group) or the observed amount of flange flattening (equivalent to a G_f of more than 45 g on some australites); (3) the cometary focus-accretion hypothesis (LYTTLETON, 1963), since this requires that the entry be vertical in the range $6 < V_i$ (km/sec) < 10, a range which would not produce anywhere near the amount of ablation observed on the high-ablation group; and (4) an origin from Antartica (COHEN, 1962), since such an origin also would not produce the observed amount of ablation. Origin directly from the Moon, however, would correspond to entry velocities slightly above 11 km/sec, and to any angle in the range $0·07 < \sin \gamma_i < 1$ between the overshoot limit and vertical entry; and such an origin is compatible with the aerodynamic evidence. It may be noted that the trajectories determined for the 13 australites in the high-ablation group and the 26 in the low-ablation group are much the same as those determined previously (CHAPMAN and LARSON, 1963) from analysis of individual buttons in the Baker collection, and that the end conclusion of lunar origin is precisely the same.

In regard to the hypothesis of tektite origin from some place on Earth, emphasis is placed on the monstrous aerodynamic obstacle to the flight of liquid drops through the atmosphere. Our experimental results have shown that drops of fused material of tektite size would be disrupted by an aerodynamic pressure differential no greater than that produced by a breath of air blown from a man's mouth (*ibid.*, p. 4321). Since it has been established that the tektites were formed molten, then cooled to a rigid state and later entered the Earth's atmosphere, an extraordinary contradiction is encountered in postulating that molten drops have flown unmolested through, and exited from, the Earth's atmosphere with velocity sufficient to overspread Australasia. This contradiction, which has been discussed in greater detail previously (*ibid.*, pp. 4318–4321), constitutes the most fundamental aerodynamic evidence for rejecting the hypothesis of tektite origin from the Earth, or from any other atmosphere shrouded planet. Recently ZÄHRINGER (1963) reported the detection of Earth atmosphere gases in the bubbles of certain tektites from Indochina and the Philippines but this does not mean that tektites were formed in the Earth's atmosphere; there is no real evidence that the atmosphere could not seep into such bubbles during their many thousands of years on Earth, while there is ample physical and observational evidence that molten tektites could not pass through the atmosphere.

PART III. MOON TO EARTH TRAJECTORIES

Inasmuch as the physical evidence from aerodynamics points to the Moon as the place of tektite origin, and the petrographic evidence points to impact as the mechanism of tektite formation, it is relevant to investigate both the probability of random trajectories going from the Moon directly to Earth, and the geographic landing patterns which might be expected of lunar impact ejecta. From a vantage point on

the Moon, the Earth's projected area subtends a solid angle that is only 1/15,000 of the 4π steradians subtended by the entire celestial sphere. This simple geometric consideration has long misled many scientists to the expectation that this minute fraction would represent the approximate probability of hitting the Earth from the Moon. Moreover, the Earth's diameter subtends a linear angle of only 2° from the Moon, and this simple consideration similarly has lead to the additional expectation that debris ejected from the Moon would overspread the entire Earth's surface, rather than only a limited fraction or proportions comparable to a tektite strewnfield. Shortly after the Moon was first suggested by VERBEEK (1897) as a possible source of tektites, and intuitive expectation immediately was voiced by others that such an origin seemed too improbable to be reasonable. Similarly, shortly after meteoritic impact on the Moon was suggested by NININGER (1943) as the mechanism of sending the tektites to Earth, the intuitive expectation was voiced that such a mechanism would be incompatible with the observed tektite distribution. Recently UREY (1962) has voiced both of these expectations without documentation by calculations of Moon to Earth trajectories. In the sections which follow these intuitive expectations are replaced by results from digital calculations.

No attempt is made herein to compute Moon to Earth trajectories to an astronomical accuracy. Instead the motion of a tektite is computed for a simplified Earth–Moon–Sun model that is adequately realistic for two limited objectives: (1) an evaluation of the probability of direct Moon to Earth trajectories and (2) a determination in the light of present knowledge about hypervelocity impact ejecta, of the order of magnitude of Earth areal spread over which the principal portion of such ejecta might land. For these limited objectives, the following approximations have been made: spherical Moon (1738 km radius, 1/81·31 of Earth mass) orbiting within the ecliptic plane in a circle 384,405 km distant from the Earth (6378 km radius including atmosphere) which is revolving about an axis perpendicular to the ecliptic. These approximations are expected to yield good results insofar as concerns such things as the probability of Earth hits from the Moon, and the probability of various angles of entry into the atmosphere. The results pertaining to Earth landing patterns of lunar ejecta are regarded as valid only as regards the order of magnitude of their areal spread. The precise patterns formed when lunar ejecta land on Earth would depend upon many things not considered in the simplified model, such as the angle of the Earth's axis relative to the lunar plane (this can vary $\pm 28°$, $\pm 23°$ of which are due to the inclination of the Earth's polar axis to the ecliptic, and $\pm 5°$ of which are due to the inclination of the lunar orbit to the ecliptic), and the librational motion of the Moon ($\pm 7°$ in lunar latitude and $\pm 8°$ in lunar longitude).

A novel feature of the present computations is the use of an analytical aiming parameter in minimizing the computation time. Most random trajectories from the Moon would wildly miss the Earth, and these are readily determined in advance by computing, by a patched conic method, the geocentric perigee for any given combination of lunar latitude φ, lunar longitude λ, elevational ejection angle β measured from the local zenith, and azimuthal ejection angle δ measured from the local lunar east (lunar "east" is taken as true celestial east, not the inverted east often used by astronomers). The machine program automatically predetermines trajectories which would have a perigee far from the Earth and computes in detail only those cases which

will go to the general vicinity of the Earth. With the use of this aiming parameter it has been practical to make computations for a number of craters and with a rather fine mesh of systematically varied increments in the elevational and azimuthal angles of ejection.

PROBABILITY OF DIRECT MOON TO EARTH TRAJECTORIES

Ten rather prominent rayed craters on the Moon have been selected for a study of Moon to Earth trajectories. The location of these lunar craters, and an arrow indicating the approximate direction in which ejecta would leave in order to have the greatest probability of landing on Earth are illustrated in the sketch of Fig. 23. Six of these craters are in maria, and four in continental areas. From each crater 504 "shots" were followed for each value of ejection velocity: at a given zenith angle β the azimuthal angle δ was varied full circle in 5° increments (72 different δ values), and β was then varied in 5° increments from 30 to 60° (7 different β-values). Eight values of the ejection velocity V_E were selected, so that the number of trajectories studied for each crater is $72 \times 7 \times 8 = 4032$.
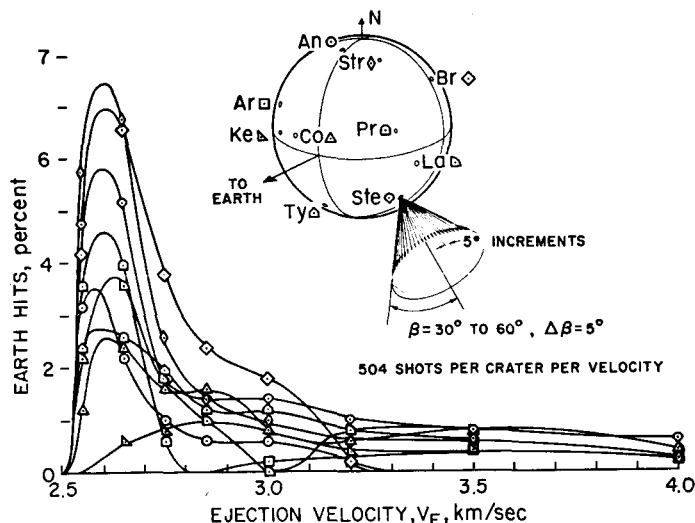

Fig. 24. Probability of direct Moon to Earth trajectories.

At certain velocities the fraction of trajectories which goes directly to the Earth is surprisingly large. For some craters (e.g. Bruno and Strabo) it is as high as about 1/15, as may be seen from the probability curves presented in Fig. 24. Such a value is very much greater than the value 1/15,000 assumed by UREY (1962), simply because of the large effect of the Earth's gravitational field in curving, then focusing, and finally pulling trajectories into a collision path with the Earth. Only for an infinite ejection velocity would the fraction 1/15,000 be applicable, since in this extreme limit the trajectories are straight lines, and intuitive expectations of probability based on the solid angle subtended by the Earth at the Moon's distance would become valid considerations.

A calculation of the over-all probability, expressed as the mass fraction of lunar crater ejecta which lands on Earth relative to the total mass which escapes the Moon,

can be made if the variation of ejected mass m_E with ejection velocity is known. In recent hypervelocity impact experiments, GAULT, SHOEMAKER and MOORE (1963) have determined this variation for cratering in basalt. Their results in the velocity range of interest can be approximated by m_E proportional to $V_E{}^n$, where n is approximately 3. Such a variation, when combined with the computational results of Fig. 24, yields the following values for the integrated mass-average probability P_m that lunar escape ejecta will go directly to Earth:

Crater	P_m per cent
Anaxagoras	0·7
Aristarchus	0·13
Bruno	1·6
Copernicus	0·9
Kepler	0·4
Langrenus	0·9
Proclus	0·7
Stevinus	1·5
Strabo	1·6
Tycho	1·0

Curiously enough, Bruno, which is situated on the back side of the Moon (103°E selenographic longitude) has a probability as high as any of the craters on the front side. This provides a good example of the precariousness involved in employing intuitive expectation, rather than digital calculation, in the study of Moon to Earth trajectories. The average value of P_m for the ten craters is 0·9 per cent, while the average value for the entire lunar surface is 0·5 per cent. This latter value was determined from computations wherein the lunar surface was divided into equal area meshes; the value of β was held constant at 45° and the δ increments were 30° and 45° (these two δ increments yielded similar results). It is emphasized that this over-all lunar average of $P_m = 0·5$ per cent, or 1/200, is much higher than the value of 1/15,000 which was obtained by neglecting the attraction of the Earth's gravitational force. This attraction results in a strong geocentric focusing of trajectories leaving the Moon.

    To this author the most impressive example encountered thus far of the dominating effect of the Earth's gravitational field in gathering up lunar ejecta and focusing it into its fold is provided by the crater Strabo. From this crater, at an elevational angle $\beta = 45°$ and at an ejection velocity $V_E = 2·55$ km/sec, a remarkably wide variation in azimuth angle can be tolerated without missing the Earth: ejecta leaving anywhere within an angular dispersion of 45° in azimuth, from $\delta = 280°$ to $\delta = 325°$, goes directly to the Earth, always landing in a rather narrow belt between 27°S and 41°N latidude as measured relative to the lunar plane. When such circumstances are recognized, it should not be surprising, as shown in the section which follows, that a jet of only several degrees dispersion, such as issues from hypervelocity impact craters, would not spread all over the Earth as has been intuitively expected in the past.

GEOGRAPHICAL SPREAD OF LUNAR-RAY EJECTA

Computations have been made of the approximate areal extent over which crater ejecta from a lunar ray would be distributed on the Earth's surface. For each of the ten rayed craters, reference values of β_0 and δ_0 were determined which would yield trajectories intercepting the Earth in the latitude range of Australasia. Both δ and β were then varied individually by constant amounts, $\Delta\delta = 2°$ and $\Delta\beta = 2°$, and additional computations made of the geographical pattern traced out for various ejection velocities. An incremental dispersion in azimuth of $\Delta\delta = 2°$ would encompass
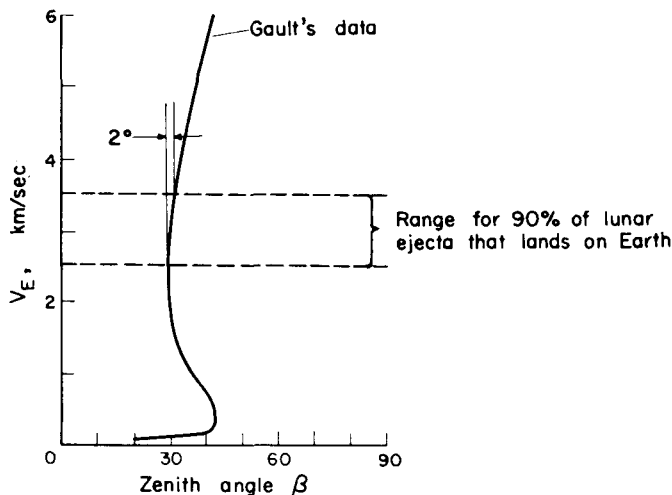

Fig. A.

the angular spread of most lunar rays; and, according to the available impact-crater experiments, an incremental dispersion in elevation of $\Delta\beta = 2°$ would represent the spread of the principal portion of lunar crater ejecta that lands on Earth. Gault's experimental results show that, as material spews from a crater, the zenith angle β varies systematically with ejection velocity. In the velocity range 3·5 to 2·5 km/sec, which encompasses approximately 90 per cent of the lunar escape ejecta that lands on Earth (Fig. 24), his experiments show β to be remarkably constant, varying no more than about 2°. These circumstances are sketched above. The 2° increments selected for angular dispersion of ejecta from a tektite-producing event, therefore, correspond to observational evidence of lunar rays and to experimental evidence from hypervelocity cratering.

It is not known how differences in scale, in impact velocity, and in target material between a lunar impact and Gault's impact experiments would affect the over-all curve of V_E versus β. Consequently, it is not assumed herein that the same values of β as measured by Gault would exist for ejecta from the Moon; but it is assumed that the same order of magnitude of the variation in β with V_E, over the V_E range of interest, would exist between the laboratory and the lunar impacts.

Although the Earth subtends an angle of about 2° from the Moon, a dispersion of 2° in either δ or β ordinarily does not spread lunar ejecta from one limb of the

Earth to the other, because of a focusing effect of the Earth's gravitational field. Some representative results illustrating the focusing effect are presented in Figs. 25 to 27. The solid curves indicate the landing paths traced out by the ejecta as the velocity is continuously decreased while β and δ are held constant. For the craters
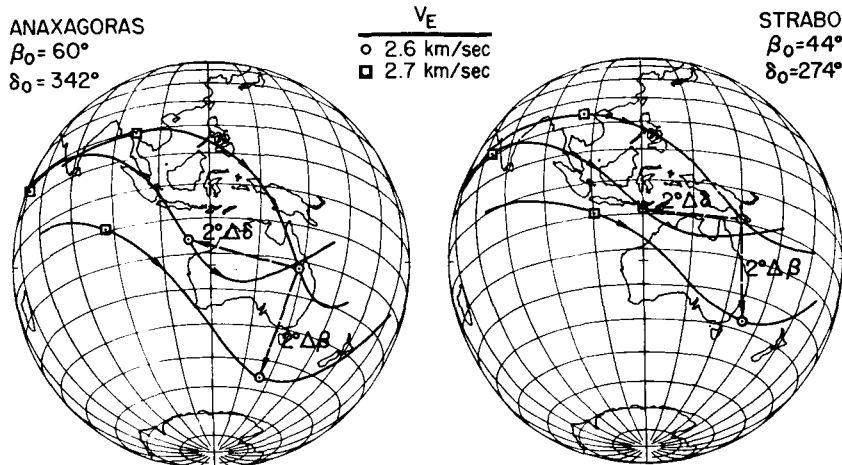

Fig. 25. Landing paths for 2° variation in lunar azimuth (δ) and zenith (β) ejection angle; Anaxagoras and Strabo.
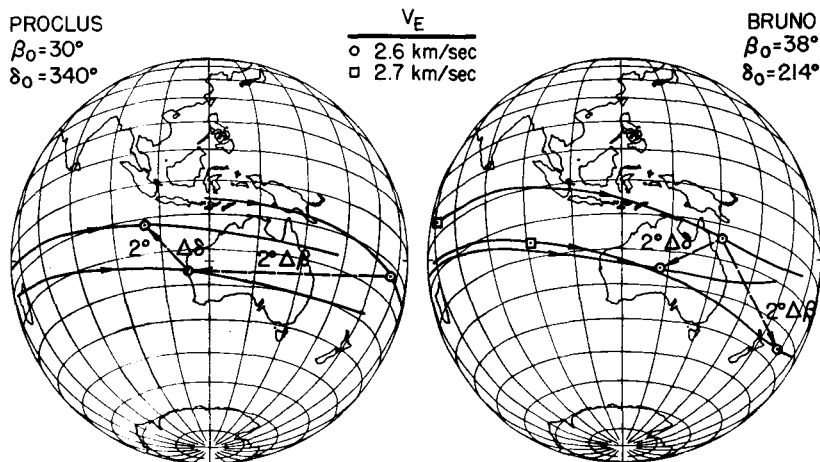

Fig. 26. Landing paths for 2° variation in lunar azimuth (δ) and zenith (β) ejection angle; Proclus and Bruno.

Anaxagoras and Strabo (Fig. 25) it is seen that a 2° variation in δ and β at the Moon would displace the landing position only about 30° of arc, on Earth's surface, or about one-sixth of the circumferential distance from limb to limb. For the craters Proclus and Bruno (Fig. 26) similar variations would spread ejecta over a rather narrow latitude belt, but over a wide stretch of longitude. For the craters Copernicus and Tycho the landing patterns are quite different (Fig. 27), and extend over an areal spread no greater than the order of magnitude of the Australasian tektite

strewnfield. In general each crater has its individual landing pattern for any given $V_E(\beta)$ relationship. However, because of the inclination of the Earth's axis to the lunar orbital plane, and of the precessional variation in this inclination, the true crater landing pattern will vary with ejection time during the lunar month, and with the ejection time during the 26,000-year period of the Earth's precession. Consequently, the present computations of landing patterns, which utilize a simplified
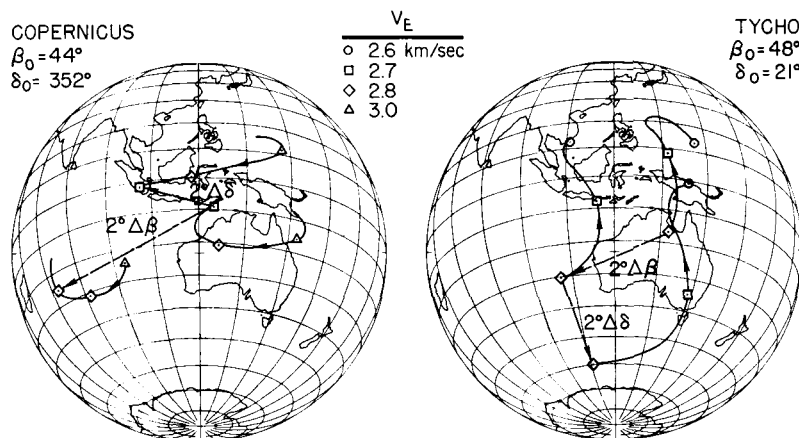

Fig. 27. Landing paths for 2° variation in lunar azimuth (δ) and zenith (β) ejection angle; Copernicus and Tycho.

Earth–Moon model, provide only a rough indication of the areal spread of lunar ray ejecta over the surface of the Earth. To this extent the above calculations are regarded as showing that there is no basic incompatibility between the order of magnitude of the spread on Earth of Australasian tektites and that of 90 per cent of the escape ejecta from a lunar ray that happens to leave the Moon along a trajectory heading towards Earth.

It is interesting to compare one qualitative feature of the landing paths for the various craters with the corresponding feature deduced earlier from studies of tektite shape. As noted previously, the high-temperature portion of impact ejecta landed in Australia, and the low-temperature portion in southeast Asia. Since the higher temperature material presumably would have been ejected at the greater velocity, it is to be expected that, as time progressed and the lunar ejection velocity decreased, the landing path of the Australasian tektites traced from the southerly latitude of Tasmania—northward through at least 65° of latitude to as far north as south China. The arrows on the solid curves in Figs. 25–27 indicate the direction in which ejecta land as time progresses and velocity decreases. For Anaxagoras and Strabo the traces sweep generally southeastward; for Proclus and Bruno generally eastward; for Copernicus generally westward; but for Tycho generally northward through at least the required 65° increment in latitude. It would appear worthwhile indeed to investigate in greater detail the possibility that the Australasian tektites might be "tychtites".

In the foregoing, only that portion of the lunar escape ejecta which goes directly to Earth has been considered. On a statistical basis, about 200 times as much

material would miss the Earth; and it is an important question to inquire about the ultimate fate of these misses. From the equal-area–mesh studies it has been found that, after 100 days (the arbitrary time limit for trajectory termination), about 0·6 per cent of these initial misses had returned to Earth, about one-fourth were in geocentric orbits, and about three-fourths were in heliocentric orbits. The ultimate fate of the geocentrics is subject to the progressive perturbations by the Moon, while that of the heliocentrics to those by the Earth. It would require extensive digital computations to establish with certainty the ultimate fate of the lunar escape ejecta which misses. In this regard, it is the writer's view that little is definite at present except that, *on a statistical basis*, the secondary returns to Earth would amount at least to the same order of magnitude as the direct hits, and would be dispersed thinly over the entire Earth's surface rather than concentrated over areas of continental proportions.

There are at least two reasons for viewing with great scepticism the application to tektites of any result derived from statistical considerations. First, tektite producing events are rare: the known events apparently span a period of over thirty-million years and are too few in number (only three or four) to constitute a good statistical sample. Second, it may be not common for every ray from a crater, or for every crater on the Moon, to send into space escaping ejecta that is similar to the particular tektite variety which is glassy, high in silica, and 1–10 cm in size. The known tektites are capable both of surviving atmosphere entry and enduring geological erosion; but other lunar ejecta might not be. To illustrate this point more specifically, let us suppose that the silica content of portions of the lunar crust is not high, but is as low as basalt and therefore would produce during an impact fused ejecta of much lower viscosity than tektite glass. Then, whereas a jet of fused tektite material would break up into objects of several centimeters size, a jet of low silica material would break up into much smaller objects, estimated to be of only several millimeters size. Objects of such small size and low viscosity first would be melted throughout during atmosphere entry and then would be broken up by aerodynamic forces into drops a fraction of a millimeter in size. Thus, one would not necessarily expect any recognizable remnant on Earth of low-silica lunar ejecta, except perhaps for occasional minute spherules that managed to escape dissolution by geological etching; these might be difficult to distinguish from cosmic spherules of other meteoritic origin. Likewise still other material related to the tektites, but not yet recognized as such, may be distributed over the Earth.

CONCLUDING REMARKS

Four principal observational results have emerged from studies of Australasian tektites in various collections supplemented by experiments conducted in the laboratory. These observational results are listed below, followed by a brief statement of the interpretations given to them.

(1) Tektites in southwest Australia are remarkably similar to, and essentially indistinguishable from, those in the Philippines in regard to their external shape, their specific gravity population, and their major element chemistry; yet are readily distinguished from tektites in southeast Australia on each of these three counts.

The interpretation of such observations is that separate portions of the same

melt mixture have been strewn from the southwest portion of Australia to the Philippines. This negates various hypotheses which have been advanced that the philippinites and the australites originate from different impact craters. Furthermore in the light of the recent evidence from population polygons of specific gravity and from the previous evidence of K–A age determinations, it is concluded that all of the Australasian tektites originate from a single impact crater.

(2) Australasian cores from Australia, Indonesia and the Philippines exhibit the same external sculpture as that obtained in aerodynamic ablation experiments wherein rigid tektite-glass models of core size are exposed to high rates of heat transfer: upon cooling, an aerothermal stress shell forms and spalls spontaneously from the outer surface leaving the characteristic core shape. Shell-like fragments from Java and Australia, with flow ridges on the covex side, exhibit the same internal stress patterns as fragments of aerothermal stress shell produced in the laboratory.

The obvious deduction from these observations is that all of the Australasian tektites descended into the Earth's atmosphere in the form of rigid glass objects that were ablated by aerodynamic heating during their hypervelocity flight. Subsequent to their fusion and formation by impact heating, therefore, even the largest Australasian tektites spent enough time in space to cool by radiation to a rigid state prior to entering the Earth's atmosphere and being subjected to severe aerodynamic heating. Insamuch as the spontaneous spallation of the thin aerothermal stress shell removes the principal aerodynamic evidence from the tektite, this offers an explanation as to where the aerodynamic evidence is for most tektites, and why such evidence has not generally been recognized in the past. This observational and experimental evidence also constitute proof that the worm-like grooves found selectively on the spalled front side of Australasian cores are not directly aerodynamic in origin, but are the result of some terrestrial phenomenon, presumably etching, which has acted selectively on the spalled surfaces after the tektites landed on Earth.

(3) The primary shapes of Australasian tektite cores change progressively from smoothly rounded objects (usually figures of revolution), universal in southeast Australia, to an inter-mixture with increasing proportions of rather angular or irregularly shaped objects in southwest Australia, Indonesia, and the Philippines. The prevalence of teardrop shapes and larger tektites in southeast Asia relative to southeast Australia is in harmony with laboratory experiments which show that the larger sizes and the teardrop shapes are associated with an increase in the viscosity of the glass corresponding to a decrease in temperature—at the time of its disruption.

The interpretation given to these results is that the higher temperature portion of the crater ejecta descended over southeast Australia and the lower temperature portions were strewn progressively over the areas of southwest Australia, then northward through Indonesia and on to the northern extremities of the Australasian strewnfield.

(4) Thin sections of tektites when viewed under cross-polarized light clearly reveal that the depth of penetration of thermal stresses and the thickness of the aerothermal stress shell is considerably less for javanites than it is for australites.

From these observations it is deduced that the javanites were subjected to higher rates of heating for shorter durations than were the australites, and have entered the atmosphere at steeper angles.

In addition to the results deduced directly from the observations and experiments summarized above, this study has produced several results from calculations of atmosphere-entry phenomena and of Moon to Earth trajectories. The reliability of the ablation calculations, it should be noted, has been established by numerous experiments in the aerodynamic laboratory. A summary of the over-all computational results is given below, followed by a brief interpretation of their significance:

(a) Calculations of the entry trajectories of Victoria australites as determined from the amount of ablation, the ring-wave formation, and the degree of flange flattening are compatible with an origin from the Moon; these calculations do not involve uncertainties about pre-entry turning, and they make allowances from direct experimental observations of the effect of body forces on the ring-wave spacing.

The obvious significance of a lunar origin, when viewed in the light of the many chemical similarities between tektite composition and average Earth crust composition, and in the contrasting light of the dissimilarities between the composition of the Earth and other celestial objects (namely, the meteorites and the Sun), leads to the expectation that the origin of the Earth's crust and the Moon's somehow are intimately interconnected. This situation stands in evident contradiction to the principal idea about the Moon's origin as advanced by UREY (1962a and previous papers referred to therein), who believes the Moon to be a primary object composed of chondritic-like, not tektite-like, material which long ago was accidently captured by the Earth. At present the author sees no way of reconciling the aerodynamic evidence as to tektite origin with the expectations of geochemists who believe that the Moon cannot possibly be the origin of tektites.

(b) The calculated probability of lunar escape ejecta going directly to the Earth depends considerably on the velocity of ejection and the selenographic position of origin: the probability can be as high as 1/15 for some craters at some velocities; on a basis of a mass average over all velocities, the probability is approximately 1/60 for these craters, and 1/200 for the entire Moon.

The significance of such results is that they remove one of the "objections" to a lunar origin for tektites which often has been raised in the past; namely, that the probability for trajectories going from the Moon directly to the Earth is too small. Previous estimates which have yielded a value of approximately 1/15,000 for this probability represent an oversimplifying premise of straight-line trajectories, and yield a probability several orders of magnitude too low because of the neglect of the dominating influence of the Earth's gravitational field in gathering in and focusing lunar escape ejecta onto its surface.

(c) A jet of material issuing from a lunar crater within an azimuthal dispersion commensurate with the width of the lunar rays, and within an elevational dispersion commensurate with that indicated by recent impact experiments, would be spread over a fraction of the Earth's surface.

The significance of this result is that it eliminates another objection which often has been raised to the idea of a lunar origin of tektites; namely, that such an origin would be expected to spread crater ejecta all over the Earth's surface rather than over dimensions comparable with those of the known tektite strewnfields.

It is not suggested that all questionable points about the idea of lunar tektite origin can be explained adequately at present. What ultimately happens to the

199/200 of the lunar escape ejecta which does not directly hit the Earth is unknown. The fate of the misses is connected with the question of whether or not tektites are typical of the lunar surface, or representative of only a fraction. Based upon the present evidence, it is expected that ejecta sufficiently low in silica, for example, would not be capable of forming large enough primary shapes, or a glass high enough in viscosity, to survive atmosphere entry (except in the form of small droplets). Extensive digital calculations would be required to provide an adequate explanation of what the ultimate fate is of the lunar ejecta which initially misses the Earth. The calculations made to date indicate that at least the same order of magnitude of mass as that which goes directly from the Moon to the Earth will later be captured by the Earth. Such secondary returns presumably would be distributed essentially uniformly over the Earth's surface. To date, no rigorous documentation is known of stray material related to the Australasian tektites that has been found in a location that is grossly removed, say, on the opposite side of the Earth from the areas of the known tektite strewnfields. But this circumstance does not mean that such strays are not present on Earth.

From a synthesis of the over-all evidence a picture of the event and the processes which produced the Australasian tektites has been reconstructed as follows: The event was initiated by the impact of a large meteoroid on the lunar surface which formed a crater estimated from total tektite mass and probability considerations to be in the range from several to the order of 100 km diameter. Two separate stages involving different physical processes are envisioned, both of which are relevant to the formation of tektites. The first stage is one of violence and intense pressure, in which various component rocks of the lunar crust are mixed, compressed, heated, and fused as they forcibly are moved in the same manner as a fluid is moved when subjected to extremely high pressures. During this stage the fused mass is bounded on one side by a compressional wave propagating into the lunar crust, and is accelerated en masse to high velocities before leaving the crater. Judging from impact experiments, masses of fused material are spewed in discrete jets at various places around the circumference of the crater, with each jet being confined to a small azimuthal dispersion. The time scale of this intense pressure stage is the order of seconds. It is pictured that the heating is the greatest in the early portions of this stage, wherein the propagating wave is strongest, and that, as the propagating wave decays and moves material outward from the impact center, the intensity of heating and the velocity of injection progressively decrease. As soon as the fused material is jetted from the surface of the Moon, however, a second stage of physical processes begin, since this material is then suddenly exposed to the vacuum of space. In the absence of external forces the masses of molten material disrupt into myriads of blobs through their own internal eddying motions coupled with the disrupting processes of boiling, outgassing, and perhaps the shattering experience of passing for a brief instant through a feeble blast of gases produced by volatilization in the earliest stage of impact. Once launched into space, surface tension is the only constraining force tending to maintain the shape of a given mass of glass. The duration of this second stage—the stage of blob formation and reshaping—would last the order of several to tens of minutes, depending upon the size of the blob. This stage would be terminated in space when the material solidified to a rigid glassy state. The processes

taking place in this second stage determine the character of the primary shapes of the tektites. Since the reshaping process takes place in a vacuum, it is possible for essentially perfect spheres, as well as other very delicate hollow forms, to be produced. It is pictured, therefore, that the jet of material leaving the Moon is comprised of a trail of progressively varying shapes and sizes. At the head would be clusters of nearly spherical shapes which were heated to the highest temperatures and given the highest velocities of ejection. These would be followed by clusters which were broken up at a somewhat higher viscosity and formed thereby less regular shapes that generally were larger than the spherical objects. These, in turn, were trailed or partially intermixed with the teardrop forms, and the large chunky tektite material, which represent the portion with the lowest temperature and highest viscosity of formation of the group. The transit time during travel from the Moon to the Earth would be the order of several days (2·5 days is a typical time) and by this time the jet string, which may have been quiet compact at the Moon, would have been dispersed to transverse dimensions comparable to those of continents on the Earth. The spherical forms would land first over the regions of southeast Australia and would be followed later by landings of the less regular primary shapes in southwest Australia and then still later by landings over Indonesia and northward on up to southeast Asia and the Philippines. The angles of descent into the atmosphere would be much steeper for the objects which fell in Indonesia than for those which fell in southeast Australia. Such a picture provides an explanation of how it is possible for one portion of a melt mixture to land over southwest Australia and another portion of the same mixture to land 5000 kilometers away in the Philippines; and it is also easy to understand how it is possible for the specific gravity populations in Java and in Australia to be much closer to each other than are various populations in different areas of Australia.

It is to be noted from the trajectory studies presented herein that it also is possible for material to be ejected from the Moon and exhibit the required overall landing pattern. Ejecta from the crater, Tycho, for example, would spread from the southern latitudes in a generally north direction across the equator to modest northerly latitudes as the velocity of the ejected material decreases. Craters which exhibit landing patterns of this nature obviously warrant more detailed investigation as possible origins of the Australasian tektites.

APPENDIX A

ANALYSIS AND EXPERIMENTAL EVALUATION OF EFFECT OF BODY FORCES ON RING-WAVE SPACING

A realistic experimental evaluation of the dependence of ring-wave spacing on body forces requires that both geometric similarity and mechanical similarity exist between the wind-tunnel model and the tektite in flight. That geometric similarity has in fact been achieved is clear from Fig. 14 wherein photographs of glycerin glass during ablation are compared with two australites (S.A.M. 625 from Charlotte Waters at the top, and U.M.G.D. 2575 from Tasmania below). These ablation experiments with glycerin glass were conducted by Mr. George Lee, who also has made measurements of the ring-wave spacing from photographic records of the ablation process. That mechanical similarity also has been achieved between wind tunnel and flight may be seen from a short computation of the corresponding ratio of body to aerodynamic forces. In keeping with the established procedures of experimental aerodynamics, it is not necessary to duplicate the dimensional forces, but only their appropriate dimensionless

ratio. The body forces appear solely in the momentum equation for the flowing glass layer

$$\frac{\partial}{\partial y}\left(\mu\,\frac{\partial u}{\partial y}\right) = \frac{dp}{dx} - \rho a\,\frac{x}{R_F} \tag{1}$$

which expresses the balance of shear forces (left side) with pressure and body forces (right side). In this equation y is measured normal to the surface, x and the corresponding velocity component u are measured parallel to the surface, μ is the viscosity of the glass, p the pressure, ρ the glass density, and a is the accelerational body force per unit mass; $a = -C_D\rho_\infty V_\infty{}^2 A/2m$ in flight, $a = -g$ in a vertical wind tunnel blowing upwards, and $a = +g$ in one blowing downwards, where ρ_∞ is the ambient air density, V_∞ the flight velocity, A the projected frontal area, m the tektite mass, and g the Earth gravitational force per unit mass. The pertinent dimensionless ratio of interest is

$$\frac{\text{Body forces}}{\text{Aerodynamic forces}} \equiv \frac{F_B}{F_A} = -\frac{\rho a x}{\dfrac{dp}{dx}\,R_F} \tag{2}$$

In hypervelocity flight $dp/dx \approx -2\rho_\infty V_\infty{}^2 x/R_F{}^2$, and in our subsonic vertical wind tunnels $dp/dx \approx -2\cdot2\rho_\infty V_\infty{}^2 x/(D/2)^2$, where D is the model diameter, and where $\rho_\infty V_\infty{}^2 = 2(p_s - p_\infty)$ in subsonic flow. By making the various substitutions it follows that

$$\frac{F_B}{F_A} \approx \begin{cases} -\dfrac{\rho R_F}{4(m/C_D A)} & \text{for hypervelocity flight conditions} \\[4mm] -\dfrac{\rho g(D/2)^2}{4\cdot4(p_s - p_\infty)R_F} & \text{for wind-tunnel conditions blowing vertically upward} \end{cases} \tag{3}$$

A further substitution in equation (3) of the appropriate numerical values of R_F, m and A for the Victorian australite buttons of the size analysed herein (base radius from 0·8 cm to 1·2 cm) yields values of F_B/F_A in the range from $-0\cdot4$ to $-0\cdot6$. For models in the wind tunnel, the values of F_B/F_A are varied by varying $(p_s - p_\infty)$, and are reversed in sign by inverting the wind tunnel. The two ablation configurations at the top left in Fig. 14 correspond to a F_B/F_A ratio of about $-0\cdot7$ and $-0\cdot9$, and represent somewhat more severe body forces than is appropriate for the Victoria buttons. These particular conditions, however, would correspond to the most extreme examples encountered among australites. That the values of this pertinent ratio in our wind-tunnel experiments corresponds to the range encountered by the australites might have been anticipated from the striking congruence of geometric shape which has been achieved between these laboratory experiments with glycerin glass, and the product of tektite flight through the atmosphere. With geometric and mechanical similarity established we now are in a position to evaluate with confidence the influence of body forces on the ring-wave spacing.

Experiments on the ablation of glycerin glass have been conducted in two wind tunnels: one blowing vertically upward producing $F_B/F_A < 0$, as in flight, and one blowing vertically downward producing $F_B/F_A > 0$. Under such conditions the ratio F_B/F_A has been varied over the range from $-0\cdot9$ to $+0\cdot3$, which includes both the range of Victoria australite buttons $-0\cdot4 < F_B/F_A < -0\cdot6$, and the range of our arc-jet experiments with tektite glass ablation $-0\cdot02 < F_B/F_A < 0$. In Fig. 15 the domain of the first ring wave, in terms of D_1/R_F, is plotted as a function of $p_s - p_\infty$ (in hypersonic flight p_∞ is negligible relative to p_s and customarily is disregarded, but in these low-speed wind-tunnel tests p_∞ must be included). The two sets of data for upward and downward directed streams are seen to be virtually identical for $p_s - p_\infty > 0\cdot006$ atm. In this range the values of R_F and D produced during ablation are such that F_B/F_A would cover the range from about $-0\cdot1$ to $0\cdot1$. Thus, in the range $-0\cdot1 < F_B/F_A < 0\cdot1$ there is no measurable effect of body forces on the first ring-wave diameter. The arc-jet data of Fig. 13, therefore, correspond to conditions of negligible body forces. At the extreme left portion of the data for the upward directed jet, the square data symbols at 0·0021 atm and 0·0020 atm correspond to the two photographs in Fig. 14 at the top and second from top, respectively. We already have seen that these represent F_B/F_A ratios of $-0\cdot7$ and $-0\cdot9$, respectively. At the same values of $p_s - p_\infty$, the circle data symbols correspond to $F_B/F_A = +0\cdot3$. Values for $F_B/F_A = 0$ would be in between. It follows that the effect of body forces in flight ($F_B/F_A < 0$) at a given stagnation pressure, is to produce

ring waves of somewhat smaller diameter than in the case of negligible body forces. The variation in F_B/F_A from $+0.3$ to -0.9 produces a contraction of ring-wave diameter which is equivalent to that produced when $p_s - p_\infty$ is changed by about a factor of two. A conservative factor of 2.0 in pressure would more than account for a variation from 0 of the arc-jet data to the extreme of -0.6 for the Victoria australites, and such a factor is employed herein to obtain a lower limit on p_{s_f} in flight.

APPENDIX B

Vapor Pressure of Tektite Glass

At the Second International Tektite Symposium two greatly different views were expressed as to the magnitude of the vapor pressure of tektite glass. In a paper presented by Dr. L. Walter, the temperature–pressure relationship for incipient bubbling of tektite glass was determined, and this interpreted as the vapor pressure. In experiments conducted at the Ames Research Center by Mr. F. Centolanzi, the rate of vaporization of tektite glass was measured relative to that of silica—a material whose vapor pressure is known to an accuracy adequate for ablation calculations. The table which follows illustrates the extraordinarily large difference between the vapor-pressure function $p_v(b)$ determined from *bubbling* observations by Walter, and the vapor-pressure function $p_v(\dot{m})$ determined from *rate of vaporization* (mass loss, $\dot{m}$) measurements by Centolanzi.

T, °K	$p_v(b)$, atm	$p_v(\dot{m})$, atm
1900	0·34	0·000013
2300	1·0	0·0025

The differences between the two functions are so great, in fact, that there is no difficulty in telling from ablation experiments which of the two is more appropriate for use in ablation calculations. Three independent tests are made in this appendix by comparing calculated results for various vapor-pressure functions with experimental measurements of (1) the surface temperature during ablation, (2) the ablation rate, and (3) the mass loss during an ablation experiment.

When tektite glass suddenly is exposed to an arc-jet stream, the surface temperature increases rapidly with time and attains a steady-state value within about 6–8 sec. In our experiments (CHAPMAN and LARSON, 1963) the energy radiated from the stagnation point E_r was measured continuously as a function of time, and is presented here for convenience in terms of the equivalent black-body temperature, or "brightness" temperature, T_b, defined as $T_b = (E_r/\sigma)^{1/4}$, where σ is the Stefan–Boltzmann constant. The actual surface temperature T_w is related to the brightness temperature, and the emissivity ϵ, through the relation $T_b = T_w\epsilon^{1/4}$. During ablation T_w exceeds T_b by about 200–300°C. For comparison with the experiments, calculations have been made for a variety of vapor pressure functions, including various multiples of $p_v(\dot{m})$ as well as the function $p_v(b)$ determined by Walter. In the table which follows measured values of T_b (to the nearest 10°) are compared with values computed for different vapor-pressure functions. The test conditions for these experiments corresponded to stagnation conditions of: enthalpy 1370 cal/g, pressure 0·35 atm, heating rate 86 cal/cm²sec, and radius of curvature 0·95 cm.

Experimental data		Calculated results	
Model	T_b, °K	Vapor pressure	T_b, °K
STG1B	2010	$0.1\,p_v(\dot{m})$	1950
STG1A	1990	$p_v(\dot{m})$	1950
A231A	1860	$10p_v(\dot{m})$	1940
A286	2020	$100p_v(\dot{m})$	1910
		$1000p_v(\dot{m})$	1830
Average	1970	$p_v(b)$	1530

In comparison to the average temperature measured, namely 1970°K, the values computed for vapor pressures within a factor of 10 from $p_v(\dot{m})$ are seen to be in reasonable agreement, but the values computed for $p_v(b)$ are about 440° too low. This means that $p_v(b)$ is much higher than the true vapor pressure

of tektite glass, since there is no possibility for an error in the experiments as large as 440°. Consequently, if $p_v(b)$ is used in aerodynamic calculations of tektite ablation, the computed temperatures will be much too low, the viscosity much too high, the ablation much too small, and the mass loss by vaporization much too high. The experimental measurements described below show that these circumstances do in fact exist.

Probably the most important aerodynamic calculation, as far as the determination of tektite entry trajectories is concerned, is the computation of the rate of aerodynamic ablation. The available experimental data on tektite ablation (CHAPMAN and LARSON, 1963) have determined the rate of ablation for test conditions at the stagnation point of: enthalpy 2700 cal/g, pressure 0·24 atm, heating rate 156 cal/cm²sec, and radius of curvature 0·95 cm. Measurements were made on two australite models, on one rizalite model, and on one model constructed of synthetic tektite glass. A comparison is made in the following table of the measured steady-state ablation rates with the corresponding calculated values for the different vapor pressure functions:

| | Experimental data | Calculated results | |
Model	dy_s/dt, cm/sec	Vapor pressure	dy_s/dt, cm/sec
AA10	0·064	$0·1\,p_v(\dot{m})$	0·061
AA152	0·065	$p_v(\dot{m})$	0·058
R258	0·076	$10p_v(\dot{m})$	0·047
ST72H	0·068	$100p_v(\dot{m})$	0·032
Average	0·068	$p_v(b)$	0·020

In comparison to the average value of the measured ablation rate, namely 0·068 cm/sec, the calculated values for a vapor pressure of $0·1\,p_v(\dot{m})$ and of $p_v(\dot{m})$ are in reasonably good agreement; that is, within the order of 10 per cent, but the calculations for a vapor pressure of $10\,p_v(\dot{m})$ or greater are in poor agreement with the experiments. The vapor pressure of tektite glass, therefore, cannot be greater than about two or three times $p_v(\dot{m})$. The calculated ablation rate for $p_v(b)$ is only one-third of the experimental value, and this is a direct proof that the vapor-pressure function $p_v(b)$ will yield grossly incorrect results if used in aerodynamic calculations. (At the Tektite Symposium E. Adams presented some ablation calculations based on $p_v(b)$.)

The third test from aerodynamic ablation experiments is provided by the integrated amount of vaporization; this quantity readily is measured by weighing a model both before and after an ablation experiment. Such measurements provide an excellent check on the vapor pressure, since the rate of vaporization and the mass loss vary sensitively with the vapor pressure. In our experiments, many runs the order of 8 sec duration were made and the mass loss by ablation carefully measured. The test conditions for these experiments were: enthalpy 2330 cal/g, pressure 0·37 atm, heating rate 175 cal/cm²sec, and radius of curvature 0·95 cm. In making calculations of the mass loss for a given model it is necessary to make allowance for the variation in vaporization rate over the front face of the model. The ratio of stagnation-point vaporization $\dot{m}_s$ to the average vaporization rate $\dot{m}_{ave}$ was determined experimentally for models of silica, and this same ratio applied for the models constructed of tektite glass. Such a procedure yields results which are good to about a factor of 2 in mass loss. In the table which follows the experimental values of mass loss Δm (in milligrams) are compared with the corresponding calculated values for various vapor-pressure functions.

In comparison to the average value of mass loss, namely 1·0 mg, it is seen that the computed value for the function $p_v(\dot{m})$ is in agreement to within the factor of 2 to which the measurements are trusted. It is also clear that computations based upon the function $p_v(b)$ yield vaporization rates which are too high by a factor of over 100. These experiments show that the correct vapor pressure to use in ablation calculations cannot be significantly greater than $p_v(\dot{m})$, and may be as much as a factor of 2 or 3 less. * There is no chance that in our balance measurements 0·1 g weights were mixed up with 0·001 g weights. Aerodynamic calculations using the vapor-pressure function $p_v(b)$ obviously will be greatly in error.

---

* For this reason computations of the lower boundary for $y_s = 1·1$ cm in Fig. (20a) have been based on $p_v = 0·5\,p_v(\dot{m})$, and the upper boundary for $y_s = 1·3$ cm on $p_v = p_v(\dot{m})$.

Experimental data		Calculated results	
Model	Δm, mg	Vapor pressure	Δm, mg
AA14	1·1	$0·1\,p_v(\dot{m})$	0·1
15	0·6	$p_v(\dot{m})$	2·1
21	1·0	$10\,p_v(\dot{m})$	15·
23	0·9	$100\,p_v(\dot{m})$	31·
S72V	1·4		
SMA	1·4		
SJU	1·3		
S1CA	1·2		
S72AF	0·8		
Average	1·0	$p_v(b)$	120·

In addition to the three experimental tests provided by the laboratory measurements of ablation phenomena, there is an observational test which is significant to apply. Some of the australite buttons were nearly perfect spheres before entry into the atmosphere, and now possess a volume of flange material (melted during flight) that nearly fills out the volume of the missing spherical segment in front of the central core (*ibid.*, Fig. 9). From these observations, it is certain that melting, and not vaporization, was the principal mechanism through which ablation proceeded during entry into the atmosphere. As noted previously (*ibid.*, pp. 4431–4432), the fraction of vaporized material relative to the total ablated, as calculated for the australite entry conditions for the vapor-pressure function $p_v(\dot{m})$, is the order of 0·25 at the stagnation point. This would correspond to the order of 10 per cent vaporization for the entire front face; that is, to ablation mainly by melting—in agreement with the australite evidence. If the calculations are made for the vapor-pressure function $p_v(b)$, however, the calculated proportions are over 99 per cent vaporization (because $p_v(b)$ is much too high) and less than 1 per cent melting. Such calculated results manifestly are incorrect; hence, calculations about the entry trajectories of the australites which are based upon the vapor-pressure function $p_v(b)$ will be grossly unrealistic.

In the author's view there is a rather simple physical explanation why the bubble-pressure function $p_v(b)$ does not represent the true vapor pressure of tektite glass. It is to be remembered that Walter determined $p_v(b)$ by observing the pressure–temperature conditions under which bubbles begin to appear in tektite glass; the gas which was forming the bubbles was not analysed. Bubbles formed as tektite glass is heated need not be composed purely of tektite vapor; in fact, the first ones formed are not expected to be composed of tektite vapor, but, instead, partly of the gases which have been dissolved within the glass and which come out of solution as the glass is heated, and partly from impurities more volatile than tektite glass. Under such circumstances, the observation of bubbles forming in tektite glass would be no more significant to the boiling temperature of tektite material than the observation of bubbles forming in soda water would be to the boiling temperature of water.

9

REFERENCES

ADAMS ERNST W. (1963) Aerodynamic analysis of tektites and their hypothetical parent bodies. Chapter 7 of *Tektites* (Ed. J. O'Keefe). University of Chicago Press, Chicago.

BAKER GEORGE (1962) The largest known australite and three smaller specimens from Warralakin, Western Australia. *J. Roy. Soc. W. A.* **45**, 12–17

BARNES VIRGIL E. and PITAKPAIVAN KASET (1962) Origin of indochinite tektites. *Proc. Nat. Acad. Sci.* **48** (6) 947–955.

CHAO E. C. T. (1963) The petrographic and chemical characteristics of tektites. Chapter 3 of *Tektites* (Ed. J. O'Keefe), pp. 51–94. University of Chicago Press, Chicago.

CHAPMAN DEAN R. (1960) Recent re-entry research and the cosmic origin of tektites. *Nature, Lond.* **188** (4748) 353–355.

CHAPMAN DEAN R. and LARSON HOWARD K. (1963) On the lunar origin of tektites. *J. Geophys. Res.* **68** (14) 4305–4358.

CHAPMAN DEAN R., LARSON HOWARD K. and SCHEIBER LEROY C. (1964) Population polygons of tektite specific gravity for various localities in Australasia. *Geochim. et Cosmochim. Acta* **28**, 821.

COHEN ALVIN J. (1962) Asteroid-impact hypothesis of tektite origin III. The southeast Asian strewn fields. *Proceedings of the Third International Space Science Symposium, Washington.* North Holland, Amsterdam.

GAULT DONALD E., SHOEMAKER EUGENE M. and MOORE HENRY J. (1963) Spray ejected from the lunar surface by meteoroid impact. NASA TN D-1767.

HARDCASTLE H. (1926) The origin of australites: plastic sweepings of a meteorite. *J. Sci. Technol. N.Z.* **8** (2) 65–75.

KOHMAN TRUMAN P. (1958) Are tektites extra-solar system meteorites? *Nature, Lond.* **182**, 252–253.

LYTTLETON R. A. (1963) A cometary mechanism for the formation of tektites. *Proc. Roy. Soc.* **A272** (1351) 467–480.

NININGER H. H. (1943) The Moon as a source of tektites. *Sky & Telesc.* **2** (4) 12–15.

O'KEEFE JOHN A. (1963) The origin of tektites. Chapter 8 of *Tektites* (Ed. J. O'Keefe). University of Chicago Press, Chicago.

SCHNETZLER C. C. and PINSON W. H. JR. (1963) The chemical composition of tektites. Chapter 4 of *Tektites* (Ed. J. O'Keefe), pp. 95–129. University of Chicago, Chicago.

TAYLOR S. R. (1962) The chemical composition of australites. *Geochim. et Cosmochim. Acta* **26**, 685–722.

UREY HAROLD C. (1962) Origin of tektites. *Science* **137**, 746–747.

UREY HAROLD C. (1962a) Origin and history of the Moon. *Physics and Astronomy of the Moon* (Ed. Z. Kopal). Academic Press, New York.

VERBEEK R. D. M. (1897) *Glaskögels van Billiton*, p. 235. Jaarboek van het Mijnwesen in Nederlandiss Oostindie, Amsterdam, 20 Jahrg.

ZÄHRINGER J. (1963) *K–A-measurements of tektites*. Paper presented at Second International Symposium on Tektites, Pittsburgh, Pa., 5–7 Sept. 1963.